

**MODELING AND ANALYSIS OF MAGNETOHYDRODYNAMIC FREE
CONVECTION TURBULENT FLUID FLOW PAST A VERTICAL INFINITE POROUS
PLATE**

KEMBOI CHERUIYOT WESLEY

**A Thesis Submitted to the Board of Graduate Studies in Partial Fulfillment of the
Requirements for Conferment of the Degree of Master of Science in Applied Mathematics
of the University of Kabianga**

Department of Mathematics, Actuarial and Physical Sciences

School of Science and Technology

University of Kabianga

OCTOBER 2023

DECLARATION AND APPROVAL

DECLARATION

I declare that this thesis is my original work and has not been presented before for the conferment/award of any degree or diploma in this or any other Institution.

Signature_____

Date_____

Kemboi Cheruiyot Wesley

PGC/AM/0002/17

APPROVAL:

This thesis has been presented with our approval as university supervisors.

Signature_____

Date_____

Wilys O. Mukuna, PhD

Department of Mathematics, Acturial and Physical Sciences,

University of Kabianga

Signature_____

Date_____

Rotich John Kimutai, PhD

Department of Mathematics, Acturial and Physical Sciences,

University of Kabianga

ABSTRACT

Magnetohydrodynamic (MHD) as an important field of study has developed over several years since its first experiment by Michael Faraday in 1832. The study is very significant in a number of ways including Biomedical sciences, engineering, Geophysics, astrophysics, Power generation among many others. There has been challenges of communications, security, power electric outages, medical issues among many others that need to be addressed. In this study, two dimensional hydro magnetic free convective flow of an incompressible viscous and electrically conducting fluid flow that is turbulent and past a vertical infinite porous plate is considered. The effect of induced magnetic field arising as a result of fluid motion that is electrically conducting is also taken into account. A mathematical model of MHD free convection fluid flow that is turbulent and past a vertical infinite porous plate is developed. The flow is impulsively started after which the analysis of the flow problem is carried out and modeled using conservation of mass, conservation of energy and conservation of momentum equations. The arising nonlinear partial differential equations are then solved using the explicit finite difference scheme. Obtained results are presented graphically and the effects of flow parameters on velocities and temperature profiles discussed. Many researchers have done investigations on magnetohydrodynamics but in spite of all these, fluid flow that is turbulent past a vertical infinite porous plate has not received much attention. Little has been done on the porous media and other non-dimensional parameters for a turbulent flow past a vertical infinite porous plate. Simulation of the discretized equations were done using MATLAB. The impacts of flow parameters on velocities and temperature profiles such as Grashof number (Gr), Magnetic parameter (M), Hall parameter (m), Prandtl number (Pr) and Turbulent prandtl number (Pr_t) analyzed. It is evident from the results that during both the cooling and heating of the plate ($Gr > 0$ and $Gr < 0$), the primary velocity decreases with decrease in Hall parameter, m , and increased magnetic parameter, M . It also decreases during cooling of the plate as the Prandtl number, Pr , is increased and even during the heating of the plate as the Prandtl number, Pr , is decreased. For $Gr > 0$ and $Gr < 0$, the secondary velocity decreases with decrease in Hall parameter, m , and increase in magnetic parameter, M . It also decreases during cooling of the plate as the Prandtl number, Pr is increased and also during heating of the plate as the Prandtl number, Pr is decreased. The results also shows that there is no significant effect on temperature profile during both cooling and heating of the plate as the Hall parameter is decreased. There is also no significant change during the cooling of the plate as the magnetic parameter is increased and even during the heating of the plate as the magnetic parameter is decreased. It is also evident that there is a decrease in temperature profile, θ , when the Prandtl number is increased in both the cooling and Heating of the plate.

COPYRIGHT

No part of this thesis may be produced, stored in any retrieval system or transmitted in any form mechanically, photocopying, recording or otherwise without prior permission from the researcher or the University of Kabianga.

© Kemboi Cheruiyot Wesley

DEDICATION

To my loving parents, Paul Nyalilei and Ruth Nyalilei together with my wife Abigael and my son Enock for their tireless support throughout my studies.

ACKNOWLEDGMENTS

I sincerely thank the Almighty GOD for His love, grace together with the physical and mental strength throughout my studies. Indeed, all glory and Honor belongs to Him. I acknowledge the wonderful work did by my supervisors, Dr. Willys Mukuna and Dr. John Rotich for their sacrifice, guidance and support during my Master program at the University of Kabianga. I thank my lecturers too for their wonderful support in shaping my knowledge that has really helped me in writing this thesis without forgetting the library staff for their wonderful support especially on the use of library resources, without them it would have been difficult for me. I also acknowledge support given to me by my parents and my wife for their prayers and encouragement throughout my studies. They have been the source of my strength in my studies. I also thank my colleagues Siele, Joyce and Elizabeth for the several discussions we held that has bore fruits of success. They have been an encouragement to me. I thank the University of Kabianga for giving me the opportunity to pursue this course. Lastly, I want to thank every other person I may not have mentioned but supported me throughout my studies, may God bless you abundantly. Thank you.

TABLE OF CONTENTS

DECLARATION AND APPROVAL	ii
ABSTRACT	iii
COPYRIGHT	iv
DEDICATION	v
ACKNOWLEDGMENTS	vi
TABLE OF CONTENTS	vii
LIST OF FIGURES	x
LIST OF ABBREVIATIONS	xii
LIST OF SYMBOLS	xiii
CHAPTER ONE	1
INTRODUCTION	1
1.1 Overview	1
1.2 Background of the study	1
1.2.1 Fluid dynamics concepts.....	1
1.3 Statement of the problem	3
1.4 Objectives of the study.....	4
1.4.1 General objective	4
1.4.2 Specific objectives	4
1.5 Significance of the study.....	4
1.6 Assumptions.....	5
CHAPTER TWO	6
LITERATURE REVIEW	6
2.1 Introduction.....	6
2.2 Review of related literature.....	6
2.3 Identification of the Knowledge gap.....	10
CHAPTER THREE	11
RESEARCH METHODOLOGY	11
3.1 Introduction.....	11
3.2. Conservation Equations	11
3.2.1 Continuity Equation.....	11

3.2.2. Conservation of Momentum Equation.....	13
3.2.3. Energy Conservation Equation	15
3.3. Turbulence and Time Averaged Equations.....	16
3.3.1. Time-Averaged Continuity Equation for Turbulent Flow	17
3.3.2. Time-Averaged Momentum Equation	18
3.3.3. Time-Averaged Energy Equation	20
3.4 Electromagnetic Equations	21
3.4.1. Maxwell’s Equations	21
3.4.2. Ohm’s Law.....	22
3.5 Non- dimensional parameters	23
3.5.1 Reynolds Number, Re	23
3.5.2 Prandtl Number, Pr	23
3.5.3 Grashof Number, Gr	24
3.5.4 Time Parameter, Rt	24
3.5.5 Eckert Number, Ec	25
3.5.6 Magnetic Parameter, M	25
3.5.7 Turbulent Prandtl Number, Prt	25
3.6 Method of Solution	25
CHAPTER FOUR.....	28
RESULTS AND DISCUSSION	28
4.1 Introduction.....	28
4.2 Mathematical model.....	28
4.3 Non-dimensionalization.....	34
4.4 Prandtl Mixing Length Hypothesis.....	38
4.5 Boundary And Initial Conditions.....	40
4.6. Explicit Finite Difference Scheme.....	40
4.7 Stability of Explicit Finite Difference Scheme	42
4.8 Discussion of Results.....	42
4.8.1 Cooling of the Plate	42
4.8.2 Heating of the Plate.....	51
4.9 Validation of results.....	61

CHAPTER FIVE	62
SUMMARY, CONCLUSIONS AND RECOMMENDATIONS	62
5.1 Introduction.....	62
5.2 Summary	62
5.3 Conclusions.....	62
5.4 Recommendations.....	64
5.5 Suggestions for further Research.....	64
REFERENCES.....	65
APPENDICES	70
Appendix I: MATLAB CODE.....	70
Appendix II: Clearance to commence field work	72
Appendix III: Publication	73

LIST OF FIGURES

Figure 3.1: Finite Difference Grid Mesh.....	27
Figure 4.1: Schematic Diagram of the Fluid flow.....	30
Figure 4.2: Primary velocity and Hall parameter for cooling of the plate.....	43
Figure 4.3: Primary velocity and Magnetic Prameter for cooling of the plate.....	44
Figure 4.4: Primary velocity and Prandtl number for cooling of the plate.....	45
Figure 4.5: Secondary velocity and Hall parameter for cooling of the plate.....	46
Figure 4.6: Secondary velocity and Magnetic parameter for cooling of the plate.....	47
Figure 4.7: Secondary velocity and Prandtl number for cooling of the plate.....	48
Figure 4.8: Temperature profile and Hall parameter for cooling of the plate.....	49
Figure 4.9: Temperature profile and Magnetic parameter for cooling of the plate.....	50
Figure 4.10: Temperature profile and Prandtl number for cooling of the plate.....	51
Figure 4.11: Primary velocity and Hall parameter for Heating of the plate.....	52
Figure 4.12: Primary velocity and Magnetic Prameter for Heating of the plate.....	53
Figure 4.13: Primary velocity and Prandtl number for Heating of the plate.....	54
Figure 4.14: Secondary velocity and Hall parameter for Heating of the plate.....	55
Figure 4.15: Secondary velocity and Magnetic parameter for Heating of the plate.....	56
Figure 4.16: Secondary velocity and Prandtl number for Heating of the plate.....	57

Figure 4.17: Temperature profile and Hall parameter for Heating of the plate.....58

Figure 4.18: Temperature profile and Magnetic parameter for Heating of the plate.....69

Figure 4.19: Temperature profile and Prandtl number for Heating of the plate.....60

LIST OF ABBREVIATIONS

MHD	Magnetohydrodynamics
N-S	Navier-Stoke's Equations
CFD	Computational Fluid Dynamics
PDEs	Partial differential equations

LIST OF SYMBOLS

H	Magnetic field intensity, (Wb/m^2)
B	Magnetic flux density, (Wb/m^2)
J	Current density vector
E	Electric field (Vm^{-1})
H_0	Constant magnetic field intensity, Wb/m^2
u, v, w	Velocity components in the x, y , and z direction respectively, m/s
u', v', w'	Fluctuating components of velocity
$\bar{u}, \bar{v}, \bar{w}$	Mean velocities
a	Acceleration, (m/s^2)
Q	Heat, (J)
W	Work, (J)
p	Fluid pressure, N/m^2
g	Acceleration due to gravity, m/s^2
t	Time, s
T	Absolute temperature, K

C_p	Specific heat at constant pressure of the fluid, $J/kg/K$
Re	Reynolds number
L	Characteristic length, m
M	Magnetic parameter
Pr	Prandtl number
Gr	Grashoff number
Ec	Eckert number
Rt	Time parameter
μ	Coefficient of viscosity, kg/ms
ρ	Fluid density, kg/m^3
α	Coefficient of thermal diffusivity, m^2 / s
ν	Coefficient of kinematic viscosity, m^2 / s
σ	Electrical conductivity, $\Omega^{-1}m^{-1}s$
β	Coefficient of thermal expansion, K^{-1}

CHAPTER ONE

INTRODUCTION

1.1 Overview

In this chapter, the history of Magnetohydrodynamics (MHD) in connection with the concept of free convection fluid flow is discussed together with the description of the terms that are used. Statement of the problem is also given together with the objectives, significance of the study and the assumptions made.

1.2 Background of the study

MHD has developed over so many years after its first experiment by Michael Faraday in 1832. However, turbulent fluid flow in MHD remains one of the unresolved areas in engineering, astrophysics, geophysics and medicine. The fundamental concept of MHD is that magnetic fields can induce currents in a moving fluid that is electrically conducting, Kwanza *et al* (2010). The particles of this fluid can move from one point to another whenever there is difference in heat energy. Particles with a lot of heat energy in a fluid will always move and take the place of a fluid with less heat energy because particles in a fluid move faster when heated than when they are cold resulting to convection. Fluid flows are either turbulent or laminar but turbulent fluid flow is of interest in this study.

1.2.1 Fluid dynamics concepts

Convection is therefore mechanism of heat transfer through a fluid in the presence of bulk fluid motion. Convection can either be forced or free. Forced convection occurs when a fluid is forced to flow by an external force. Free convection on the other hand occurs when the fluid flow is initiated by buoyancy forces. In this case, there exist density gradient between materials as a result

of buoyancy forces. When a fluid density remains constant throughout the flow, the fluid is considered to be incompressible or referred to as Newtonian fluid. When the fluid density varies in the flow, the fluid is compressible or referred to as non-Newtonian fluid.

Fluid flow can be categorized as either laminar or turbulent. Laminar flow is always characterized by complete orderliness of fluid particles for instance when oil or honey is poured into a container. Turbulent flow on the other hand is characterized by fluctuation in velocity or pressure quantities for instance flow through turbines or flowing water through a tap with high pressure. In free convection flows, Grashof number, Gr , is important in that flows with $Gr > 10^9$ are turbulent while those in the range of $10^3 < Gr < 10^6$ are considered laminar, (Holman, 2010).

Reynolds number, Re , is a parameter which determines whether a fluid flow is laminar or turbulent. Low Re indicates laminar flow while a high Re indicates turbulent flow. Since fluid flow that is turbulent is of interest in this case, these parameters are great of great significance.

A streamline refers to a continuous line within a fluid such that the tangent at each point is the direction of the velocity vector at that point. It is a curve c that is drawn in the flow field such that the fluid velocity is along the direction of the tangent of the curve. A fluid flow is described as steady fluid flow when the velocity at each point is independent of time and the flow pattern is the same at each instant. It is referred to as unsteady fluid flow when the flow pattern is time dependent, therefore flow pattern varies at each instant. A path line refers to the trajectory of an individual element of a fluid. Thus, the streamlines show how all particles are moving at a given instant while path lines show how a given particle is moving at each instant. Therefore, when the motion is steady, the path lines coincide with the streamline.

Porous medium on the other hand is a permeable solid with a network of interconnected pores that is filled with fluid (liquid or gas). The network of pores is assumed to be continuous as it is for the case of a sponge. Some of the examples of porous materials are rocks, bones, soils, cement slabs, ceramics, foam among many others.

Considering magnetic field effect on fluid flow, it is important to understand the physical mathematical framework that concerns the dynamics of magnetic fields in electrically conducting fluids that is referred to as magnetohydrodynamic (MHD). It is the field of study which takes into consideration the properties of electromagnetism and fluid mechanics to describe the flow of electrically conducting fluid, (Kwanza 2010).

Considering the law of electromagnetism, any conductor moving within a magnetic field generates an electric current known as Hall current. A magnetohydrodynamic free convection fluid that is turbulent and past an infinite vertical porous plate is studied considering the Hall current and discussing the impacts of non-dimensional parameters on velocities and temperature profiles.

1.3 Statement of the problem

Among the several research investigations, the combined effects on free convection, turbulence, and porous medium to the MHD flow on an infinite vertical plate has not been done in one study hence the motivation to carry out this research. This study is on modeling and analysis of magnetohydrodynamic free convection turbulent fluid flow past a vertical infinite porous plate.

1.4 Objectives of the study

1.4.1 General objective

To Model and analyze a MHD free convection fluid flow that is turbulent past a vertical infinite porous plate with Hall current and the effects of non- dimensional parameters on velocities and temperature profiles discussed.

1.4.2 Specific objectives

- i) To develop a mathematical model using the conservation of mass, conservation of energy and conservation of momentum equations considering a fluid flow that is turbulent and past a vertical infinite porous plate.
- ii) To solve numerically, the partial differential equations arising from the developed mathematical model.
- iii) To analyze the effect of changes in the non- dimensional parameters on the velocity and temperature profiles of the fluid.

1.5 Significance of the study

This research will be applicable in a number of ways including Biomedical sciences, engineering, geophysics, astrophysics among many other applications as discussed below:

- i) MHD has its significance in the field of medicine such as magnetic drug targeting which is a precise way of administering drugs to the affected area. This is very important in cancer research. It is also useful in magnetic devices for cell separation, adjusting blood flow during surgery, transporting bio- waste fluids among many other uses.
- ii) MHD has its significance in the field of engineering including electric power generation, electromagnetic pumping and propulsion and control of moving molten metals

It is also significant in developing space weather forecasting capability which is important for safe operation of manned spacecraft and a variety of communications, global positioning, and defense satellite systems as well as for protection against geometrically- induced electric power outages on earth.

iii) It is worth noting that MHD is also significant in the study of the earth's surface which comprises of the inner and the outer core containing a significant amount of iron. The outer core which is liquid in nature moves in the presence of magnetic field leading to the formation of eddies due to Coriolis Effect affecting the earth's magnetic field.

iv) MHD is very useful in describing astrophysical systems. These are in most cases in an unstable local equilibrium therefore requires kinematic consideration for their description within the system. For instance the sunspots result from the sun's magnetic field.

1.6 Assumptions

The following assumptions are made in this research:

- i) The fluid taken into consideration is incompressible
- ii) There are no chemical reactions or contaminants in the fluid
- iii) There is no external electric field
- iv) The fluid flow is non- relativistic.

CHAPTER TWO

LITERATURE REVIEW

2.1 Introduction

A lot of research has been undertaken in MHD therefore literature related to turbulent fluid flow, vertical infinite plate and the effects of non-dimensional parameters are reviewed in this chapter. Knowledge gap also identified.

2.2 Review of related literature

Mukuna *et al.* (2020) modeled a Hydromagnetic free convection turbulent fluid flow over a vertical infinite plate using turbulent Prandtl number. They found out that there is an increase in primary velocity whenever magnetic parameter(M) is decreased, Hall parameter increased and when Grashoff number is increased. It was also evident that secondary velocity increases when magnetic parameter (M) is decreased and decreases when Hall parameter is increased. They also found out that temperature profile decreases when magnetic parameter (M) is decreased, decreases when Hall parameter is increased and also increases when Prandtl number decreases.

Vijayalakshmi *et al.* (2018) did a research on the unsteady electrically transmitting fluid past an oscillating semi- infinite vertical plate with uniform temperature and mass diffusion under chemical reactions. They realized that heat transfer progress is enhanced with the oscillating frequency, Prandtl number and thermal Grashof number.

Odekeye and Akinrinmade (2017) did a MHD research on mixed convective heat and mass transfer flow from vertical surfaces in porous media with Soret and Dufour effects and found out that an increase in magnetic field leads to a decrease in velocity and increase in temperature.

Loganathan and Eswari (2017) did a research on natural convective flow over moving vertical cylinder with temperature oscillation in the presence of porous medium. They used the iterative tridiagonal semi-implicit finite difference method. Their results showed that whenever the permeability parameter increases, there was a corresponding increase in velocity and boundary thermal layer and decrease in concentration layer.

Mukuna *et al.* (2017b) analyzed heat and mass transfer rates of hydromagnetic turbulent fluid flow over an immersed cylinder with Hall current. They modeled the flow using conservation equations and solved the arising partial differential equations using finite difference scheme. They concluded that increasing the hall parameter increases the velocity profiles while an increase in magnetic parameter leads to an increase in temperature and concentration profiles.

Mukuna *et al.* (2017a) researched on hydromagnetic turbulent free convection fluid flow over an immersed infinite vertical cylinder, modeled their problem using conservation equations and later solved the arising partial differential equations using finite difference scheme. They found out that whenever the Hall parameter was increased, there was a corresponding decrease in secondary velocity while the primary velocity profile was not affected due to turbulence.

Kiprop (2017) did a research on an unsteady MHD flow with mass and heat transfer in an incompressible, viscous, Newtonian and electrically conducting fluid past a vertical porous plate with consideration of chemical reaction, thermal radiation and induced magnetic field. Solution of governing equations were done using finite difference scheme, that is the Crank- Nicholson method. His findings shows that velocity decreases with increasing magnetic parameter (M) and also decrease in concentration with increasing Schmidt number and chemical reaction.

Seth *et al.* (2016) studied on the effects of an unsteady free convection flow past an impulsively moving porous vertical plate with Newtonian heating and found out that fluid flow in both the primary and secondary flow directions are accelerated by the hall current, permeability of the medium, thermal buoyancy force, Newtonian heating and thermal diffusion throughout the boundary layer region while magnetic field tend to retard the fluid flow and together with hall current tend to increase the secondary skin friction. They also showed that thermal buoyancy force and thermal diffusion tend to increase the secondary skin friction. Newtonian heating tends to reduce primary skin friction but increase secondary skin friction.

Chebos *et al.* (2016) investigated an unsteady MHD free convection flow past an oscillating vertical porous plate with oscillatory heat flux and found out that there is velocity increase with decrease in suction parameter and magnetic parameter and increase with increase in Darcy number. They also found out that temperature increases with decrease in Prandtl number and increase with increase in radiation parameter and suction parameter.

Unameheswar *et al.* (2016) did numerical investigation of MHD free convection of non-Newtonian fluid past an impulsively started vertical plate in the presence of thermal diffusion and radiation absorption. Their results show that increasing magnetic field parameter decreases the velocity.

Vishnu *et al.* (2016) studied hydromagnetic asymmetrical slip flow over a vertical stretching cylinder with convective boundary on a viscous fluid and used Runge- Kutta method to solve the arising partial differential equations. They found out that whenever the velocity-slip increases and Prandtl number decreases, the normal boundary layer thickness increases.

Rajesh *et al.* (2016) investigated finite difference analysis of unsteady MHD free convective flow over a moving semi-infinite vertical cylinder with chemical reaction and temperature oscillations. They solve the arising partial differential equations using the Crank- Nicolson finite difference scheme and found out that their results were in agreement with available computations and literature.

Ravi and Sambasiva (2016) studied buoyancy induced natural convective heat transfer along a vertical cylinder under constant heat flux and were able to show that temperature of both cylinder and fluid increases along axial direction and decreases along radial direction.

Deka *et al.* (2015) researched on transient free convection flow past a vertical cylinder with constant heat flux and mass transfer and concluded that velocity and temperature increases significantly with time and that at larger times, concentration approaches steady state.

Massoud *et al.* (2015) studied the effect of magnetic field on free convection inclined cylindrical annulus containing molten potassium and found out that increasing magnetic field leads to a loss of symmetry and shape of isotherms.

Mayaka *et al.* (2014a) investigated a MHD turbulent fluid flow past a vertical porous plate and solved the governing equations using finite difference scheme and Prandtl mixing length theorem was used to handle turbulence. He found out that the Hall current, Joules's heating and mass transfer had effects on primary and secondary velocity, and also concentration and temperature profiles.

Kwanza *et al.* (2010) worked on a mathematical model of turbulent convective fluid flow past an infinite vertical plate with Hall current in a dissipative fluid and found out that an increase in hall current leads to an increase in velocity profiles.

Sarris *et al.* (2010) explained magnetic field effect on the cooling of a low-Pr fluid in a vertical cylinder in the presence of magnetic field and found out that magnetic fields has no effect at the initial stages of development of the boundary layer.

2.3 Identification of the Knowledge gap

In the above review, section 2.2, it can be noticed that indeed a lot of research has been undertaken in MHD. However, none has modeled and analyzed fluid flow that is turbulent and past a vertical infinite porous plate.

Kwanza *et al.* (2010) developed a model of a turbulent convective fluid past an infinite vertical plate with Hall current in a dissipative fluid but did not consider the porous medium. It is also noted that Chebos *et al.* (2016) investigated MHD free convection flow past an oscillating vertical porous plate with oscillatory heat flux but ignored Hall current and a vertical infinite porous plate that is not oscillating.

It is due to this therefore that a mathematical model of a MHD free convection fluid flow that is turbulent and past an infinite vertical porous plate is developed. In this study, consideration is given to the effect of porous material together with non- dimensional parameters for a fluid flow that is turbulent.

CHAPTER THREE

RESEARCH METHODOLOGY

3.1 Introduction

The general conservation equations are given in this chapter, which include the conservation of mass equation, conservation of momentum equation and conservation of energy equation. Non-dimensional parameters that are very significant in this study are also given together with the explicit finite difference scheme which is the method of solution used to solve the arising partial differential equations.

3.2. Conservation Equations

Fluid flow in fluid dynamics can be described using the conservation equations based on the conservation laws which include the law of conservation of mass, the law of conservation of momentum and the law of conservation of energy. These laws give rise to the conservation equations which include:

- i) Continuity equation
- ii) Navier- Stokes equation
- iii) Energy equation

Each of them is discussed below:

3.2.1 Continuity Equation

This equation is also referred to as conservation of mass equation. It is based on the principle of conservation of mass, which states that the mass of a body can neither be created nor destroyed.

This is given as:

$$\frac{dm}{dt} = 0 \quad (3.1)$$

Where m is the mass

Edward *et al.* (2005) derives continuity equation and gives:

$$\frac{\partial \rho}{\partial t} + \vec{\nabla} \cdot (\rho \vec{u}) = 0 \quad (3.2)$$

Where,

$$\vec{\nabla} = \frac{\partial}{\partial x} \hat{i} + \frac{\partial}{\partial y} \hat{j} + \frac{\partial}{\partial z} \hat{k} \quad (3.3)$$

Continuity equation can be given in other forms which include;

$$\frac{\partial \rho}{\partial t} + \vec{u} \cdot \vec{\nabla} \rho + \rho \vec{\nabla} \cdot \vec{u} = 0 \quad (3.4)$$

Where $\vec{u} \cdot \vec{\nabla} \rho + \rho \vec{\nabla} \cdot \vec{u}$ in equation (3.4) is the expanded form of $\vec{\nabla} \cdot (\rho \vec{u})$ in equation (3.2). Thus the mass conservation equation is given as:

$$\frac{d\rho}{dt} + \rho \vec{\nabla} \cdot \vec{u} = 0 \quad (3.5)$$

Where (3.5) is obtained by substituting the material derivative $\frac{d\rho}{dt} = \frac{\partial \rho}{\partial t} + (\vec{u} \cdot \vec{\nabla})\rho$ into (3.4).

Note that equation (3.2) is commonly used in computational fluid dynamics (CFD).

For an incompressible fluid, continuity equation in cartesian coordinate system is given as (Edward J. S. *et al.*, 2005)

$$\left(\frac{\partial \rho}{\partial t} + u \frac{\partial \rho}{\partial x} + v \frac{\partial \rho}{\partial y} + w \frac{\partial \rho}{\partial z} \right) + \rho \left(\frac{\partial u}{\partial x} + \frac{\partial v}{\partial y} + \frac{\partial w}{\partial z} \right) = 0 \quad (3.6)$$

Where u , v and w represent the velocity components x , y and z axes respectively.

For an incompressible flow, the fluid density is constant therefore

$\frac{d\rho}{dt} = 0$ and the continuity equation (3.2) reduces to

$$\vec{\nabla} \cdot \vec{u} = 0 \quad (3.7)$$

In Cartesian coordinates, the continuity equation in incompressible flow is therefore given by:

$$\frac{\partial u}{\partial x} + \frac{\partial v}{\partial y} + \frac{\partial w}{\partial z} = 0 \quad (3.8)$$

3.2.2. Conservation of Momentum Equation

This equation is also referred to as Navier-Stoke's equation (N-S) for a Newtonian fluid. The differential equation expressing the law of momentum is given by:

$$\frac{\partial(\rho \vec{u})}{\partial t} + \vec{\nabla} \cdot (\rho \vec{u} \vec{u}) = \rho f + \vec{\nabla} \cdot \sigma \quad (3.9)$$

Where ρf refers to the sum of body forces and $\vec{\nabla} \cdot \sigma$ represents the stress divergence term.

On expanding the time derivative and divergence terms and rearranging remaining terms we get:

$$\rho \left(\frac{\partial \vec{u}}{\partial t} + \vec{u} \cdot \vec{\nabla} \vec{u} \right) + \vec{u} \left[\frac{\partial \rho}{\partial t} + \vec{u} \cdot \vec{\nabla} \rho + \rho \vec{\nabla} \cdot \vec{u} \right] = \rho f + \vec{\nabla} \cdot \sigma \quad (3.10)$$

The first equation in brackets in the left-hand side of equation (3.10) represents the inertial forces per unit volume.

Since the fluid density is constant, for an incompressible flow, it implies that the term in square or closed brackets of continuity equation (3.10) is equal to zero. Thus, equation (3.10) becomes:

$$\rho \left(\frac{\partial \vec{u}}{\partial t} + (\vec{u} \cdot \vec{\nabla}) \vec{u} \right) = \rho f + \vec{\nabla} \cdot \sigma \quad (3.11)$$

Using material derivative $\frac{du}{dt} = \frac{\partial \vec{u}}{\partial t} + (\vec{u} \cdot \vec{\nabla}) \vec{u}$, the differential momentum equation takes the form:

$$\rho \frac{du}{dt} = \rho f + \vec{\nabla} \cdot \sigma \quad (3.12)$$

Where $\rho \frac{du}{dt}$ represents the inertial force

ρf represents body force and $\vec{\nabla} \cdot \sigma$ refer to surface force.

Anderson, (1991) used the definition of stress divergence to give the three components of momentum equations in cartesian coordinate system as:

$$\rho \left(\frac{\partial u}{\partial t} + u \frac{\partial u}{\partial x} + v \frac{\partial u}{\partial y} + w \frac{\partial u}{\partial z} \right) = -\frac{\partial p}{\partial x} + \rho f_x + \mu \left(\frac{\partial^2 u}{\partial x^2} + \frac{\partial^2 u}{\partial y^2} + \frac{\partial^2 u}{\partial z^2} \right) \quad (3.13)$$

$$\rho \left(\frac{\partial v}{\partial t} + u \frac{\partial v}{\partial x} + v \frac{\partial v}{\partial y} + w \frac{\partial v}{\partial z} \right) = -\frac{\partial p}{\partial y} + \rho f_y + \mu \left(\frac{\partial^2 v}{\partial x^2} + \frac{\partial^2 v}{\partial y^2} + \frac{\partial^2 v}{\partial z^2} \right) \quad (3.14)$$

$$\rho \left(\frac{\partial w}{\partial t} + u \frac{\partial w}{\partial x} + v \frac{\partial w}{\partial y} + w \frac{\partial w}{\partial z} \right) = -\frac{\partial p}{\partial z} + \rho f_z + \mu \left(\frac{\partial^2 w}{\partial x^2} + \frac{\partial^2 w}{\partial y^2} + \frac{\partial^2 w}{\partial z^2} \right) \quad (3.15)$$

Where u, v, w are the velocity components in the x, y, z directions, p is the pressure, f_x, f_y, f_z are the body forces components which include Coriolis force, gravity and electromagnetic force in the x, y, z directions. In this study we will consider only gravity and electromagnetic forces as the body forces.

3.2.3. Energy Conservation Equation

This is a scalar equation derived from the principle of thermodynamics. It is based on the first law of thermodynamics which states that the amount of heat added to the system is equal to the change in the internal energy plus the work done. This is given as:

$$dQ = dE + dW \quad (3.16)$$

The conservation of energy equation for a Newtonian fluid is given as

$$\frac{dQ}{dt} = \frac{dE_T}{dt} + \frac{dW}{dt} \quad (3.17)$$

Where $\frac{dQ}{dt}$ is the rate of change of heat

$\frac{dE_T}{dt}$ is the rate of change of internal energy at constant temperature

$\frac{dW}{dt}$ is the work done by the system.

For an incompressible fluid, the conservation of energy equation is the resultant of the First law of Thermodynamics and therefore given as:

$$\rho C_p \left[\frac{\partial T}{\partial t} + \vec{\nabla} \cdot (T\vec{u}) \right] = \vec{\nabla} \cdot (k\vec{\nabla}T) + \phi \quad (3.18)$$

Where,

p is the fluid pressure

C_p is the specific heat at constant pressure

k is the thermal conductivity

ρ is the fluid density

$$\vec{V} = \frac{\partial}{\partial x} \hat{i} + \frac{\partial}{\partial y} \hat{j} + \frac{\partial}{\partial z} \hat{k}$$

ϕ is the viscous dissipation given by:

$$\phi = 2 \left[\left(\frac{\partial u}{\partial x} \right)^2 + \left(\frac{\partial v}{\partial y} \right)^2 + \left(\frac{\partial w}{\partial z} \right)^2 \right] + \left(\frac{\partial v}{\partial x} + \frac{\partial u}{\partial y} \right)^2 + \left(\frac{\partial w}{\partial y} + \frac{\partial v}{\partial z} \right)^2 + \left(\frac{\partial u}{\partial z} + \frac{\partial w}{\partial x} \right)^2 - \frac{2}{3} \left(\frac{\partial u}{\partial x} + \frac{\partial u}{\partial y} + \frac{\partial u}{\partial z} \right) \quad (3.19)$$

u, v, w are velocity components in x, y, z directions respectively.

The conservation of energy equation in Cartesian coordinate is therefore given as:

$$\rho C_p \left[\frac{\partial T}{\partial t} + u \frac{\partial T}{\partial x} + v \frac{\partial T}{\partial y} + w \frac{\partial T}{\partial z} \right] = k \left(\frac{\partial^2 T}{\partial x^2} + \frac{\partial^2 T}{\partial y^2} + \frac{\partial^2 T}{\partial z^2} \right) + \phi \quad (3.20)$$

3.3. Turbulence and Time Averaged Equations.

Conservation equations are transformed to Reynolds averaged equations in order to govern turbulent flow. Turbulence result whenever a disturbance is induced in a laminar flow. Deriving the Reynolds equations is done by decomposing the dependent variables of the laminar flow of

conservation equations into time-mean and fluctuating components and then time averaging the entire equation.

The following are true when turbulent flow parameters are considered:

$$u = \bar{u} + u' \quad (3.21)$$

$$v = \bar{v} + v' \quad (3.22)$$

$$w = \bar{w} + w' \quad (3.23)$$

$$p = \bar{p} + p' \quad (3.24)$$

$$T = \bar{T} + T' \quad (3.25)$$

Where,

$$\bar{u} = \frac{1}{t} \int_0^t u dt \quad (3.26)$$

$$\bar{v} = \frac{1}{t} \int_0^t v dt \quad (3.27)$$

$$\bar{w} = \frac{1}{t} \int_0^t w dt \quad (3.28)$$

3.3.1. Time-Averaged Continuity Equation for Turbulent Flow

Considering continuity equation(3.8) takes the form $\frac{\partial u}{\partial x} + \frac{\partial v}{\partial y} + \frac{\partial w}{\partial z} = 0$ (3.29)

And substituting turbulent fluctuations, $u = \bar{u} + u', v = \bar{v} + v'$

And $w = \bar{w} + w'$ yields

$$\frac{\partial \bar{u}}{\partial x} + \frac{\partial \bar{u}'}{\partial x} + \frac{\partial \bar{v}}{\partial y} + \frac{\partial \bar{v}'}{\partial y} + \frac{\partial \bar{w}}{\partial z} + \frac{\partial \bar{w}'}{\partial z} = 0 \quad (3.30)$$

When equation (3.29) is integrated over $0 \rightarrow t$, it yields

$$\frac{\partial \bar{u}}{\partial x} + \frac{\partial \bar{u}'}{\partial x} + \frac{\partial \bar{v}}{\partial y} + \frac{\partial \bar{v}'}{\partial y} + \frac{\partial \bar{w}}{\partial z} + \frac{\partial \bar{w}'}{\partial z} = 0 \quad (3.31)$$

Simplifying equation (3.31) gives

$$\frac{\partial \bar{u}}{\partial x} + \frac{\partial \bar{v}}{\partial y} + \frac{\partial \bar{w}}{\partial z} = 0 \quad (3.32)$$

Equation (3.32) is the mean velocity component for mass conservation equation.

Considering equation (3.32), equation (3.30) reduces to:

$$\frac{\partial \bar{u}'}{\partial x} + \frac{\partial \bar{v}'}{\partial y} + \frac{\partial \bar{w}'}{\partial z} = 0 \quad (3.33)$$

This is the fluctuating component of velocity for turbulent flow for mass conservation equation.

For turbulent flow, mass is always conserved for both mean velocity components and fluctuating velocity components.

3.3.2. Time-Averaged Momentum Equation

Considering momentum equation in x -direction when body forces are neglected gives:

$$\frac{\partial u}{\partial t} + \left(u \frac{\partial u}{\partial x} + v \frac{\partial u}{\partial y} + w \frac{\partial u}{\partial z} \right) = -\frac{1}{\rho} \left(\frac{\partial p}{\partial x} \right) + \frac{\mu}{\rho} \left(\frac{\partial^2 u}{\partial x^2} + \frac{\partial^2 u}{\partial y^2} + \frac{\partial^2 u}{\partial z^2} \right) \quad (3.34)$$

When equation (3.29) is multiplied by u and added to equation (3.34) it yields

$$\frac{\partial u}{\partial t} + \left(\frac{\partial u^2}{\partial x} + \frac{\partial(uv)}{\partial y} + \frac{\partial(uw)}{\partial z} \right) = -\frac{1}{\rho} \left(\frac{\partial p}{\partial x} \right) + \frac{\mu}{\rho} \left(\frac{\partial^2 u}{\partial x^2} + \frac{\partial^2 u}{\partial y^2} + \frac{\partial^2 u}{\partial z^2} \right) \quad (3.35)$$

When equation (3.34) is averaged over $0 \rightarrow t$, it gives

$$\frac{\partial \bar{u}}{\partial t} + \left(\frac{\partial \bar{u}^2}{\partial x} + \frac{\partial \overline{(uv)}}{\partial y} + \frac{\partial \overline{(uw)}}{\partial z} \right) = -\frac{1}{\rho} \left(\frac{\partial \bar{p}}{\partial x} \right) + \frac{\mu}{\rho} \left(\frac{\partial^2 \bar{u}}{\partial x^2} + \frac{\partial^2 \bar{u}}{\partial y^2} + \frac{\partial^2 \bar{u}}{\partial z^2} \right) \quad (3.36)$$

But $\frac{\partial \bar{u}}{\partial t} = 0$ and substituting for $u = \bar{u} + u'$, $v = \bar{v} + v'$ and $w = \bar{w} + w'$ in equation (3.36) it yields:

$$\left(\frac{\partial (\bar{u})^2}{\partial x} + \frac{\partial \overline{(u)^2}}{\partial x} \right) + \left(\frac{\partial \bar{u}\bar{v}}{\partial y} + \frac{\partial \bar{u}v'}{\partial y} \right) + \left(\frac{\partial \bar{u}\bar{w}}{\partial z} + \frac{\partial \bar{u}w'}{\partial z} \right) = -\frac{1}{\rho} \left(\frac{\partial \bar{p}}{\partial x} \right) + \frac{\mu}{\rho} \left(\frac{\partial^2 \bar{u}}{\partial x^2} + \frac{\partial^2 \bar{u}}{\partial y^2} + \frac{\partial^2 \bar{u}}{\partial z^2} \right) \quad (3.37)$$

It can be shown that:

$$\frac{\partial (\bar{u})^2}{\partial x} = 2\bar{u} \frac{\partial \bar{u}}{\partial x} \quad (3.38)$$

$$\frac{\partial \bar{u}\bar{v}}{\partial y} = \bar{u} \frac{\partial \bar{v}}{\partial y} + \bar{v} \frac{\partial \bar{u}}{\partial y} \quad (3.39)$$

$$\frac{\partial \bar{u}\bar{w}}{\partial z} = \bar{u} \frac{\partial \bar{w}}{\partial z} + \bar{w} \frac{\partial \bar{u}}{\partial z} \quad (3.40)$$

When equation(3.38),(3.39) and (3.40) is substituted to equation (3.37) it yields:

$$\left(2\bar{u} \frac{\partial \bar{u}}{\partial x} + \frac{\partial \overline{(u)^2}}{\partial x} \right) + \left(\bar{u} \frac{\partial \bar{v}}{\partial y} + \bar{v} \frac{\partial \bar{u}}{\partial y} + \frac{\partial \bar{u}v'}{\partial y} \right) + \left(\bar{u} \frac{\partial \bar{w}}{\partial z} + \bar{w} \frac{\partial \bar{u}}{\partial z} + \frac{\partial \bar{u}w'}{\partial z} \right) = -\frac{1}{\rho} \left(\frac{\partial \bar{p}}{\partial x} \right) + \frac{\mu}{\rho} \left(\frac{\partial^2 \bar{u}}{\partial x^2} + \frac{\partial^2 \bar{u}}{\partial y^2} + \frac{\partial^2 \bar{u}}{\partial z^2} \right) \quad (3.41)$$

When equation (3.32) is multiplied by \bar{u} and subtracted from equation (3.41), the result is:

$$\left(\bar{u} \frac{\partial \bar{u}}{\partial x} + \frac{\partial \overline{(u)^2}}{\partial x} \right) + \left(\bar{v} \frac{\partial \bar{u}}{\partial y} + \frac{\partial \bar{u}v'}{\partial y} \right) + \left(\bar{w} \frac{\partial \bar{u}}{\partial z} + \frac{\partial \bar{u}w'}{\partial z} \right) = -\frac{1}{\rho} \left(\frac{\partial \bar{p}}{\partial x} \right) + \frac{\mu}{\rho} \left(\frac{\partial^2 \bar{u}}{\partial x^2} + \frac{\partial^2 \bar{u}}{\partial y^2} + \frac{\partial^2 \bar{u}}{\partial z^2} \right) \quad (3.42)$$

Rearranging equation (3.42) yields:

$$\bar{u} \frac{\partial \bar{u}}{\partial x} + \bar{v} \frac{\partial \bar{u}}{\partial y} + \bar{w} \frac{\partial \bar{u}}{\partial z} = -\frac{1}{\rho} \left(\frac{\partial \bar{p}}{\partial x} \right) + \frac{\mu}{\rho} \left(\frac{\partial^2 \bar{u}}{\partial x^2} + \frac{\partial^2 \bar{u}}{\partial y^2} + \frac{\partial^2 \bar{u}}{\partial z^2} \right) - \left(\frac{\partial \overline{(u)^2}}{\partial x} + \frac{\partial \bar{u}v'}{\partial y} + \frac{\partial \bar{u}w'}{\partial z} \right) \quad (3.43)$$

Momentum equations in the y and z-directions can be done in the same way and given as:

$$\bar{u} \frac{\partial \bar{v}}{\partial x} + \bar{v} \frac{\partial \bar{v}}{\partial y} + \bar{w} \frac{\partial \bar{v}}{\partial z} = -\frac{1}{\rho} \left(\frac{\partial \bar{p}}{\partial x} \right) + \frac{\mu}{\rho} \left(\frac{\partial^2 \bar{v}}{\partial x^2} + \frac{\partial^2 \bar{v}}{\partial y^2} + \frac{\partial^2 \bar{v}}{\partial z^2} \right) - \left(\frac{\partial \bar{v}\bar{u}}{\partial x} + \frac{\partial \overline{(v)^2}}{\partial y} + \frac{\partial \bar{v}\bar{w}}{\partial z} \right) \quad (3.44)$$

$$\bar{u} \frac{\partial \bar{w}}{\partial x} + \bar{v} \frac{\partial \bar{w}}{\partial y} + \bar{w} \frac{\partial \bar{w}}{\partial z} = -\frac{1}{\rho} \left(\frac{\partial \bar{p}}{\partial x} \right) + \frac{\mu}{\rho} \left(\frac{\partial^2 \bar{w}}{\partial x^2} + \frac{\partial^2 \bar{w}}{\partial y^2} + \frac{\partial^2 \bar{w}}{\partial z^2} \right) - \left(\frac{\partial \bar{w}\bar{u}}{\partial x} + \frac{\partial \bar{w}\bar{v}}{\partial y} + \frac{\partial \overline{(w)^2}}{\partial z} \right) \quad (3.45)$$

Equations (3.43), (3.44) and (3.45) are turbulent momentum equations for turbulent flow for an incompressible fluid in the x , y and z - directions respectively.

3.3.3. Time-Averaged Energy Equation

When the dissipative function is neglected in equation (3.20) the energy equation is given as:

$$\rho C_p \left(\frac{\partial T}{\partial t} + u \frac{\partial T}{\partial x} + v \frac{\partial T}{\partial y} + w \frac{\partial T}{\partial z} \right) = k \left(\frac{\partial^2 T}{\partial x^2} + \frac{\partial^2 T}{\partial y^2} + \frac{\partial^2 T}{\partial z^2} \right) \quad (3.46)$$

When equation (3.29) is multiplied by T and added it to equation (3.46) in component form the result is:

$$\frac{\partial T}{\partial t} + \frac{\partial(uT)}{\partial x} + \frac{\partial(vT)}{\partial y} + \frac{\partial(wT)}{\partial z} = \frac{k}{\rho C_p} \left(\frac{\partial^2 T}{\partial x^2} + \frac{\partial^2 T}{\partial y^2} + \frac{\partial^2 T}{\partial z^2} \right) \quad (3.47)$$

When equation (3.47) is averaged over $0 \rightarrow t$, it gives:

$$\frac{\partial \bar{T}}{\partial t} + \frac{\partial \overline{(uT)}}{\partial x} + \frac{\partial \overline{(vT)}}{\partial y} + \frac{\partial \overline{(wT)}}{\partial z} = \frac{k}{\rho C_p} \left(\frac{\partial^2 \bar{T}}{\partial x^2} + \frac{\partial^2 \bar{T}}{\partial y^2} + \frac{\partial^2 \bar{T}}{\partial z^2} \right) \quad (3.48)$$

But $T = \bar{T}$ Since fluctuation in temperature is neglected and $u = \bar{u} + u(t)$, $v = \bar{v} + v(t)$ and $w = \bar{w} + w(t)$, thus when this is substituted to equation (3.48) and rearranging it yields:

$$\begin{aligned} \frac{\partial \bar{T}}{\partial t} + \left(\bar{u} \frac{\partial \bar{T}}{\partial x} + \bar{T} \frac{\partial \bar{u}}{\partial x} \right) + \left(\bar{v} \frac{\partial \bar{T}}{\partial y} + \bar{T} \frac{\partial \bar{v}}{\partial y} \right) + \left(\bar{w} \frac{\partial \bar{T}}{\partial z} + \bar{T} \frac{\partial \bar{w}}{\partial z} \right) &= \frac{k}{\rho C_p} \left(\frac{\partial^2 \bar{T}}{\partial x^2} + \frac{\partial^2 \bar{T}}{\partial y^2} + \frac{\partial^2 \bar{T}}{\partial z^2} \right) - \\ \left(\frac{\partial \overline{(uT)}}{\partial x} + \frac{\partial \overline{(vT)}}{\partial y} + \frac{\partial \overline{(wT)}}{\partial z} \right) & \end{aligned} \quad (3.49)$$

Since $\frac{\partial \bar{u}}{\partial x} = \frac{\partial \bar{v}}{\partial y} = \frac{\partial \bar{w}}{\partial z} = 0$ as shown from the time- average equation and hence substituting this

into equation (3.49) yields

$$\frac{\partial \bar{T}}{\partial t} + \bar{u} \frac{\partial \bar{T}}{\partial x} + \bar{v} \frac{\partial \bar{T}}{\partial y} + \bar{w} \frac{\partial \bar{T}}{\partial z} = \frac{k}{\rho c_p} \left(\frac{\partial^2 \bar{T}}{\partial x^2} + \frac{\partial^2 \bar{T}}{\partial y^2} + \frac{\partial^2 \bar{T}}{\partial z^2} \right) - \left(\frac{\partial(\overline{uT})}{\partial x} + \frac{\partial(\overline{vT})}{\partial y} + \frac{\partial(\overline{wT})}{\partial z} \right) \quad (3.50)$$

Thus equation (3.50) is the energy equation for turbulent flow.

3.4 Electromagnetic Equations

MHD comprises of electromagnetic and fluid mechanics therefore governing equations are always taken out of electromagnetic theory and fluid mechanics. These include Maxwell's and Ohm's law equations, David (2006).

3.4.1. Maxwell's Equations

Maxwell's first equation known as curl \vec{E} equation which gives the relationship between the electric and magnetic fields is given as:

$$\vec{\nabla} \times \vec{E} = \frac{\partial \vec{B}}{\partial t} \quad (3.51)$$

Maxwell's second equation known as Maxwell's curl H is given as:

$$\vec{\nabla} \times \vec{H} = \vec{J} \quad (3.52)$$

(3.52) can be expressed in a general form as:

$$\vec{\nabla} \times \vec{H} = \vec{J} + \frac{\partial \vec{D}}{\partial t} \quad (3.53)$$

Where $\frac{\partial \vec{D}}{\partial t}$ refers to the displacement current.

Therefore the four Maxwell's equations governing electromagnetic theory are given as follows:

$$\vec{\nabla} \times \vec{E} = \frac{\partial \vec{B}}{\partial t} \quad (3.54)$$

$$\vec{\nabla} \times \vec{H} = \vec{j} \quad (3.55)$$

$$\vec{\nabla} \cdot \vec{B} = 0 \quad (3.56)$$

Equation (3.56) is Gauss' law of magnetism.

$$\vec{\nabla} \cdot \vec{D} = \rho_e \quad (3.57)$$

Equation (3.57) is Gauss' law of electricity.

3.4.2. Ohm's Law

The magnitude of the induced current for any conductor moving within the magnetic field is given as $\vec{q} \times \vec{B}$. Thus the Ohm's law expressing the current density is given as:

$$\vec{j} = \sigma \vec{E} \quad (3.58)$$

In this case, E is the effective electric field intensity and σ is the current density.

But when a conductor is moving in a magnetic field, this is given as $\vec{E} + \vec{q} \times \vec{B}$ where E is the applied electric field and $\vec{q} \times \vec{B}$ is the induced electric field. This brings equation (3.58) as:

$$\vec{j} = \sigma(\vec{E} + \vec{q} \times \vec{B}) \quad (3.59)$$

Equation (3.59) is the Ohm's law giving the current density.

3.5 Non- dimensional parameters

These are parameters that are useful in fluid dynamics and they include Reynolds Number, Re, Prandtl Number, Pr, Grashof Number, Gr, Time Parameter, Rt, Eckert number, Ec, Magnetic Parameter, M, among many others. They are introduced to the governing equations through scaling variables. This is to ensure that the solution is independent from units of any given variable.

3.5.1 Reynolds Number, Re

This is the ratio of the inertia force to the viscous force. It gives the significance of inertia and viscous forces in fluid flow.

It is used to determine whether the flow is laminar or turbulent. Low Re shows laminar flow while high Re indicates turbulent flow. It is given by:

$$\text{Re} = \frac{\rho v L}{\mu}$$

Where ρ is the fluid density,

v is the velocity scale,

L is the Length scale and

μ is the fluid viscosity Incropera, (2007)

3.5.2 Prandtl Number, Pr

This is the ratio of viscosity to the thermal diffusivity. It is given by:

$$\text{Pr} = \frac{\mu C_p}{k} = \frac{\nu}{\alpha}$$

Where $\nu = \frac{\mu}{\rho}$ is the kinematic viscosity and

$\alpha = \frac{k}{\rho C_p}$ is the thermal diffusivity coefficient.

3.5.3 Grashof Number, Gr

It is the ratio of forcing (buoyancy) force to restraining (viscous) force.

It is significant in free convection flows. Gr of over 10^9 indicates turbulent flow while Gr in the range $10^3 < Gr < 10^6$ indicates laminar flow, (Holman, 2010)

It is given by:

$$Gr = \frac{g\beta(T - T_\infty)L^3}{\nu^2}$$

g is the gravitational acceleration

β refers to the thermal expansion coefficient.

T and T_∞ are the surface and bulk temperatures respectively

L is the characteristic length and

ν is the coefficient of kinematic viscosity.

3.5.4 Time Parameter, Rt

This is a parameter characterizing the time scale of the problem with respect to flow velocity. It is defined as

$$R_t = \frac{t_0 u_0}{L}$$

3.5.5 Eckert Number, Ec

This represents a dimensionless parameter which is important in flows of high speed with significant viscous dissipation. It gives the ratio of kinetic energy to the boundary layer enthalpy.

It is given by:

$$Ec = \frac{u^2}{C_p \Delta T}$$

ΔT refers to temperature change.

3.5.6 Magnetic Parameter, M

Refers to the ratio of magnetic force to inertia force. It is given by:

$$M^2 = \frac{\text{Magnetic force}}{\text{Inertia force}} = \frac{\sigma \mu^2 H \nu}{\rho u^2}$$
$$\Rightarrow M = \sqrt{\frac{\sigma \mu^2 H \nu}{\rho u^2}}$$

3.5.7 Turbulent Prandtl Number, Pr_t

This refers to the ratio of momentum eddy diffusivity to the heat transfer diffusivity. It is given as:

$$Pr_t = \frac{\varepsilon_M}{\varepsilon_H}, \text{ where } \varepsilon_M = 2k^2 z^2 \frac{\partial \bar{v}}{\partial z}$$

3.6 Method of Solution

The arising partial differential equations shall be solved using the explicit finite difference scheme which gives the numerical approximation of the solution. And thereafter the results presented in form of graphs.

Grid mesh is considered which assumed to be a rectangular plane with the horizontal axis y and the vertical axis t . In this case, t is varied from $0 \rightarrow a$ and y is varied from $0 \rightarrow b$ with the intervals being divided into n and m each having width Δt and Δy respectively.

Given any point on the rectangular plane say (y_i, t_j) can be defined as

$$y_i = i\Delta y; i = 1, 2, 3, \dots$$

$$t_j = j\Delta t; j = 1, 2, 3, \dots$$

The given figure is an illustration of the intersections at the mesh points by the grid lines y_i and t_j

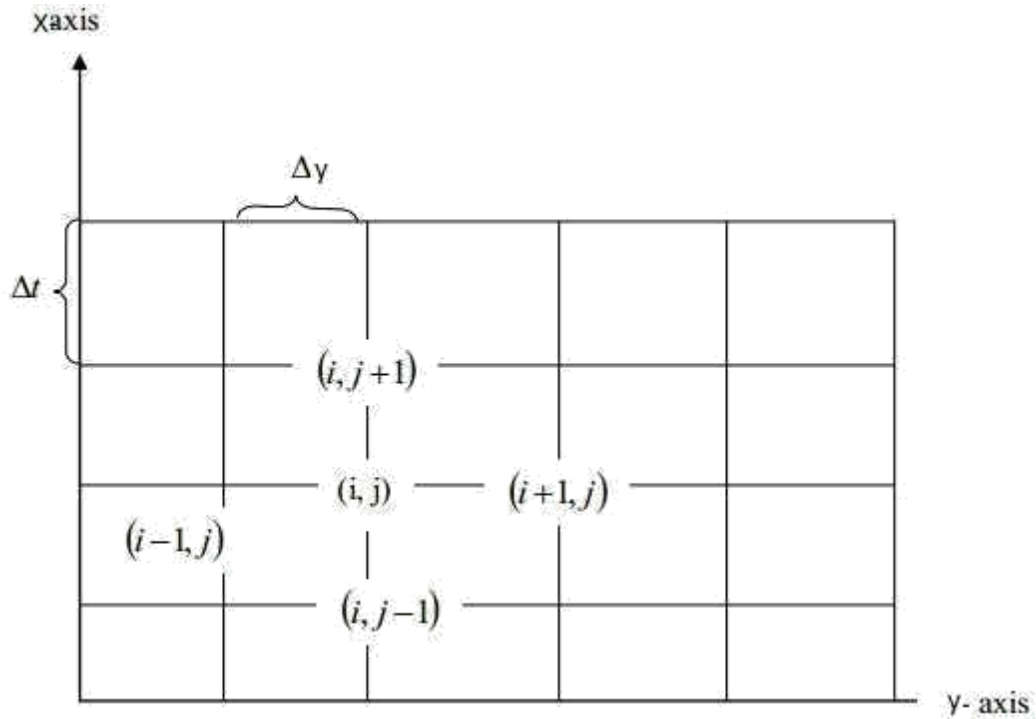


Figure 3.1: Finite difference Grid Mesh

Considering the finite difference approximation for the first and second derivatives of U with respect to y , and applying the Taylor's series expansion in variables y and t at the points

$(y_{(i+1,j)}, t_j)$ and $(y_{(i-1,j)}, t_j)$ about (y_i, t_j) we obtain:

$$U_{(i+1,j)} = U_{(i,j)} + U_{y(i,j)}\Delta y + \frac{1}{2}U_{yy(i,j)}(\Delta y)^2 + \dots \quad (3.60)$$

$$U_{(i-1,j)} = U_{(i,j)} - U_{y(i,j)}\Delta y + \frac{1}{2}U_{yy(i,j)}(\Delta y)^2 + \dots \quad (3.61)$$

$$U_{(i,j+1)} = U_{(i,j)} + U_{t(i,j)}\Delta t + \frac{1}{2}U_{tt(i,j)}(\Delta t)^2 + \dots \quad (3.62)$$

$$U_{(i,j-1)} = U_{(i,j)} - U_{t(i,j)}\Delta t + \frac{1}{2}U_{tt(i,j)}(\Delta t)^2 + \dots \quad (3.63)$$

$$\text{In this case, } U_{(i,j)} = U_{(y_i,t_j)} \text{ and } U_{y(i,j)} = \frac{\partial U_{(y_i,t_j)}}{\partial y} \quad (3.64)$$

Eliminating U_y and U_{yy} in equations (3.60) and (3.61) and also U_t and U_{tt} in equations (3.62)

and (3.63), the following set of equations are obtained.

$$\frac{\partial U_{(i,j)}}{\partial y} = \frac{U_{(i+1,j)} - U_{(i-1,j)}}{2h} + o(h^2) \quad (3.65)$$

$$\frac{\partial U_{(i,j)}}{\partial t} = \frac{U_{(i,j+1)} - U_{(i,j-1)}}{2k} + o(k^2) \quad (3.66)$$

$$\frac{\partial^2 U_{(i,j)}}{\partial y^2} = \frac{U_{(i+1,j)} - 2U_{(i,j)} + U_{(i-1,j)}}{h^2} + o(h^2) \quad (3.67)$$

$$\frac{\partial^2 U_{(i,j)}}{\partial t^2} = \frac{U_{(i,j+1)} - 2U_{(i,j)} + U_{(i,j-1)}}{k^2} + o(k^2) \quad (3.68)$$

The approximate solutions for the finite difference scheme for the differential equations are obtained using equations (3.65), (3.66), (3.67), and (3.68). Smaller values of Δt and Δy are considered to minimize the order of truncation errors.

CHAPTER FOUR

RESULTS AND DISCUSSION

4.1 Introduction

In this chapter, the governing equations for the problem are formulated. Consideration of the analysis of hydro magnetic free convection fluid flow that is turbulent and past an infinite vertical porous plate is given. The fluid being considered is electrically conducting. Conservation equations are used to modeled the problem in this chapter as stated in chapter three . The modeled governing equations are non-dimensionalised for this problem and some of the non-dimensional parameters discussed in chapter three are also introduced. The approximate numerical solution determined by the use of explicit finite difference scheme and solved by the use of MATLAB computer software. The results are presented graphically and discussed.

4.2 Mathematical model

A two-dimensional flow is considered in this study. The infinite vertical porous plate is taken to be along the x-axis and the y-axis taken to be on the horizontal whereas the z-axis normal to the plate. The fluid being considered is incompressible and viscous. A magnetic field of a high magnitude H_0 is applied perpendicularly to the direction of flow of the fluid. It is assumed that the induced magnetic field is negligible therefore $H = (0,0,H_0)$ as indicated in the schematic diagram in figure 4.1. At time $t^*>0$, the fluid is stationary and the plate starts to move impulsively in its plane with velocity U_0 and the temperature of the plate raised instantly to T_W^* and maintained constant later on.

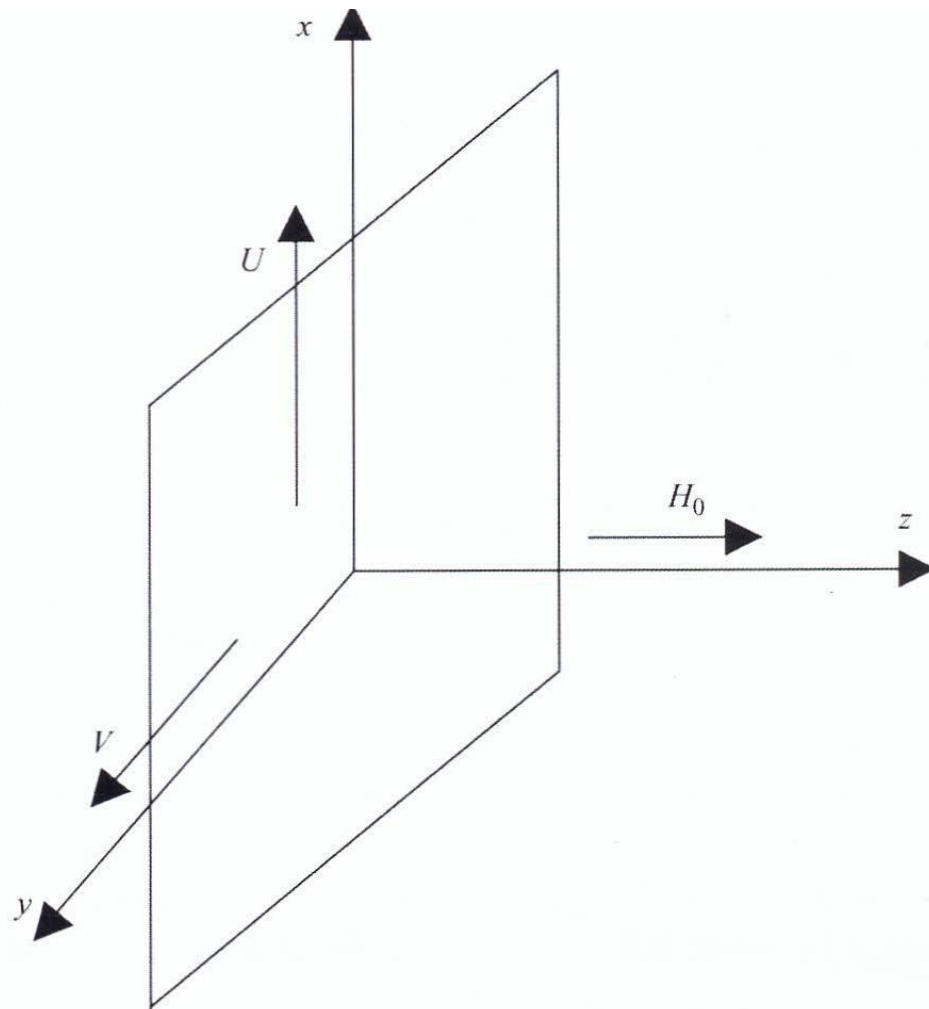


Figure 4.1: Schematic diagram for the fluid flow.

The flow is therefore governed by the following equations:

$$\frac{\partial U^*}{\partial t^*} + V^* \frac{\partial U^*}{\partial y^*} = -\frac{1}{\rho} \frac{\partial p}{\partial x} + \nu \left(\frac{\partial^2 U^*}{\partial z^{*2}} \right) - \frac{\partial(\bar{u}\bar{w})}{\partial z^*} + \rho g + \vec{j} \times \vec{B} \quad (4.1)$$

$$\frac{\partial V^*}{\partial t^*} + V^* \frac{\partial V^*}{\partial y^*} = \nu \left(\frac{\partial^2 V^*}{\partial z^{*2}} \right) - \frac{\partial(\bar{u}\bar{w})}{\partial z^{*2}} + \vec{j} \times \vec{B} \quad (4.2)$$

$$\frac{\partial T^*}{\partial t^*} + V^* \frac{\partial T^*}{\partial y^*} = \frac{k}{\rho C_p} \left(\frac{\partial^2 T^*}{\partial z^{*2}} \right) - \frac{\partial(\bar{w}\bar{T})}{\partial z^*} \quad (4.3)$$

Where,

$\nu = \frac{\mu}{\rho}$ is the kinematic viscosity

ρ Is the fluid density

ρg is the specific weight of the fluid

The initial and boundary conditions will be as follows:

$t^* < 0 : U^* = 0, V^* = 0, T^* = T_\infty^*$ everywhere

$t^* \geq 0 : U^* = 0, V^* = 0, T^* = T_\infty^*$ at $z \rightarrow \infty$

$U^* = 1, V^* = 0, T^* = T_w^*$, at $z = 0$

The change in elevation up the plate will result in the pressure gradient in the x- axis direction

therefore $\frac{\partial p}{\partial x} = -\rho_\infty g$

Thus equation (4.1) becomes:

$$\frac{\partial U^*}{\partial t} + V \frac{\partial U^*}{\partial y^*} = v \left(\frac{\partial^2 U^*}{\partial z^{*2}} \right) - \frac{\partial(\bar{u}\bar{w})}{\partial z^*} + g(\rho - \rho_\infty) + \vec{J} \times \vec{B} \quad (4.4)$$

Hollman, (2010) defined that the difference in density can be expressed in terms of volume coefficient of expansion given by

$$\beta = \frac{1}{V} \left(\frac{\partial U}{\partial T} \right)_p = \frac{1}{V_\infty} \cdot \frac{V - V_\infty}{T - T_\infty} = \frac{(\rho_\infty - \rho)}{\rho(T - T_\infty)} \quad (4.5)$$

$$\text{Thus, } \beta = \frac{\rho_\infty - \rho}{\rho(T - T_\infty)}$$

When equation (4.5) is substituted in equation (4.4), the result is:

$$\frac{\partial U^*}{\partial t^*} + V^* \frac{\partial U^*}{\partial y^*} = v \left(\frac{\partial^2 U^*}{\partial z^{*2}} \right) - \frac{\partial(\bar{u}\bar{w})}{\partial z^*} + g\rho\beta(T^* - T_\infty^*) + \vec{J} \times \vec{B} \quad (4.6)$$

The term $\vec{J} \times \vec{B}$ represents electromagnetic force therefore its components can be obtained from the equation of conservation of electric charge given by

$$\vec{\nabla} \cdot \vec{J} = 0, \text{ giving } \hat{j}_z = \text{constant where}$$

$$\vec{J} = (\hat{j}_x, \hat{j}_y, \hat{j}_z).$$

Since $\hat{j}_z = 0$ at the plate which is electrically non-conducting, this constant is assumed to be zero, therefore $\hat{j}_z = 0$ everywhere in the flow.

Cowling, (1957) gave the generalized ohm's law with Hall current effects as

$$\vec{J} + \frac{\omega_e \tau_e}{H_0} (\vec{J} \times \vec{H}) = (\vec{E} + \mu_e \vec{q} \times \vec{H} + \frac{1}{en_e} \vec{\nabla} p_e) \quad (4.7)$$

Where, $\vec{\nabla}$ = Gradient operator, given as $\vec{\nabla} = \hat{i} \frac{\partial}{\partial x} + \hat{j} \frac{\partial}{\partial y} + \hat{k} \frac{\partial}{\partial z}$

$p_e =$ Electron pressure

$\vec{E} =$ Electric field (Vm^{-1}),

$\mu_e =$ electron permeability (H/m)

$\omega_e \tau_e = m$ is the hall parameters

In this case, the ion- slip and thermoelectric effects are neglected.

Since there is no applied electric field, then

$$\vec{E} = 0 \quad (4.8)$$

If we neglect electron pressure, equation 4.7 reduces to;

$$\vec{J} + \frac{\omega_e \tau_e}{\vec{H}_0} (\vec{J} \times \vec{H}) = \sigma (\mu_e \vec{q} \times \vec{H}) \quad (4.9)$$

$$\text{Where } \vec{J} = \hat{j}_x^* + \hat{j}_y^* + \hat{j}_z^* \quad (4.10)$$

When equation (4.8) and (4.10) is substituted into (4.9), it yields:

$$\hat{j}_x^* + \hat{j}_y^* + \hat{j}_z^* + \frac{\omega_e \tau_e}{H_0} \begin{vmatrix} i & j & k \\ \hat{j}_x^* & \hat{j}_y^* & \hat{j}_z^* \\ 0 & 0 & \vec{H}_0 \end{vmatrix} = \sigma \mu_e \begin{vmatrix} i & j & k \\ u & v & w \\ 0 & 0 & \vec{H}_0 \end{vmatrix} \quad (4.11)$$

This yield,

$$\hat{j}_x^* + \hat{j}_y^* + \hat{j}_z^* + \frac{\omega_e \tau_e}{H_0} (\vec{H}_0 \hat{j}_y^* - \vec{H}_0 \hat{j}_x^* + 0) = \sigma \mu_e (V \vec{H}_0 - \mu \vec{H}_0 + 0) \quad (4.12)$$

Equation (4.12) gives:

$$\hat{j}_x^* + \omega_e \tau_e \hat{j}_y^* = \sigma \mu_e \vec{H}_0 V^* \quad (4.13)$$

$$\hat{j}_y^* - \omega_e \tau_e \hat{j}_x^* = \sigma \mu_e \vec{H}_0 U^* \quad (4.14)$$

Since $m = \omega_e \tau_e$, then

$$\hat{j}_x^* + m \hat{j}_y^* = \sigma \mu_e \vec{H}_0 V^* \quad (4.15)$$

$$\hat{j}_y^* - m \hat{j}_x^* = -\sigma \mu_e \vec{H}_0 U^* \quad (4.16)$$

Simultaneous solution of equation (4.15) and (4.16) gives

$$\hat{j}_x^* = \frac{\sigma \mu_e H_0 (m U^* + V^*)}{1 + m^2} \quad (4.17)$$

$$\hat{j}_y^* = \frac{\sigma \mu_e H_0 (m V^* - U^*)}{1 + m^2} \quad (4.18)$$

Therefore the force due to electromagnetism is given by

$$\vec{j} \times \vec{B} = \begin{vmatrix} i & j & k \\ \hat{j}_x^* & \hat{j}_y^* & 0 \\ 0 & 0 & \vec{B}_0 \end{vmatrix} \quad (4.19)$$

If \vec{B}_0 is substituted with $\mu_e \vec{H}_0$ then equation (4.19) becomes;

$$\vec{j} \times \vec{B} = \begin{vmatrix} i & j & k \\ \hat{j}_x^* & \hat{j}_y^* & 0 \\ 0 & 0 & \mu_e \vec{H}_0 \end{vmatrix} \quad (4.20)$$

Equation (4.20) also reduces to

$$\vec{j} \times \vec{B} = (\mu_e \vec{H}_0 \hat{j}_y^* - \mu_e \vec{H}_0 \hat{j}_x^* + 0) \quad (4.21)$$

It is therefore from this equation that electromagnetic force along x-axis and y-axis can be obtained from equation (4.17) and (4.18) respectively. These are given as:

$$(\vec{J} \times \vec{B})_{x^*} = \frac{\sigma \mu_e^2 H_0^2 (mV^* - U^*)}{1 + m^2} \quad (4.22)$$

$$(\vec{J} \times \vec{B})_{y^*} = - \frac{\sigma \mu_e^2 H_0^2 (mU^* + V^*)}{1 + m^2} \quad (4.23)$$

Thus, the governing equations (4.1) and (4.2) become:

$$\frac{\partial U^*}{\partial t^*} + V^* \frac{\partial U^*}{\partial y^*} = v \left(\frac{\partial^2 U^*}{\partial z^{*2}} \right) - \frac{\partial(\bar{u}\bar{w})}{\partial z^*} + g\beta(T^* - T_\infty^*) + \frac{\sigma \mu_e^2 H_0^2 (mV^* - U^*)}{1 + m^2} \quad (4.24)$$

$$\frac{\partial V^*}{\partial t^*} + V^* \frac{\partial V^*}{\partial y^*} = v \left(\frac{\partial^2 V^*}{\partial z^{*2}} \right) - \frac{\partial(\bar{v}\bar{w})}{\partial z^{*2}} + g\beta(T^* - T_\infty^*) - \frac{\sigma \mu_e^2 H_0^2 (mU^* + V^*)}{1 + m^2} \quad (4.25)$$

4.3 Non-dimensionalization

We non-dimensionalize equation (4.3), (4.24) and (4.25) using the following scaling variables in the process of Non –dimensionalisation.

$$t = \frac{t^* U_0^2}{v}, \quad z = \frac{z^* U_0}{v}, \quad y = \frac{y^* U_0}{v}, \quad U = \frac{U^*}{U_0}, \quad V = \frac{V^*}{U_0}, \quad \theta = \frac{T^* - T_w^*}{T_w^* - T_\infty^*}, \quad (4.26)$$

In this case;

The superscript (*) denotes dimensional variable.

U_0 Denotes reference velocity,

$T_w^* - T_\infty^*$ Denotes temperature difference between the surface and the free stream temperature.

When the above scaling variables are used, we obtained the following:

$$\frac{\partial U^*}{\partial t^*} = \frac{\partial U^*}{\partial U} \frac{\partial U}{\partial t} \frac{\partial t}{\partial t^*} = \frac{U_0^3}{v} \frac{\partial U}{\partial t} \quad (4.27)$$

$$\frac{\partial V^*}{\partial t^*} = \frac{\partial V^*}{\partial V} \frac{\partial V}{\partial t} \frac{\partial t}{\partial t^*} = \frac{U_0^3}{v} \frac{\partial V}{\partial t} \quad (4.28)$$

$$\frac{\partial U^*}{\partial z^*} = \frac{\partial U^*}{\partial U} \frac{\partial U}{\partial z} \frac{\partial z}{\partial z^*} = \frac{U_0^2}{v} \frac{\partial U}{\partial z} \quad (4.29)$$

$$\frac{\partial V^*}{\partial z^*} = \frac{\partial V^*}{\partial V} \frac{\partial V}{\partial z} \frac{\partial z}{\partial z^*} = \frac{U_0^2}{v} \frac{\partial V}{\partial z} \quad (4.30)$$

$$\frac{\partial T^*}{\partial t^*} = \frac{\partial T^*}{\partial \theta} \frac{\partial \theta}{\partial t} \frac{\partial t}{\partial t^*} = (T_w^* - T_\infty^*) \frac{U_0^2}{v} \frac{\partial \theta}{\partial t} \quad (4.31)$$

$$\frac{\partial U^*}{\partial y^*} = \frac{\partial U^*}{\partial U} \frac{\partial U}{\partial y} \frac{\partial y}{\partial y^*} = \frac{U_0^2}{v} \frac{\partial U}{\partial y} \quad (4.32)$$

$$\frac{\partial U^*}{\partial z^{*2}} = \frac{\partial}{\partial z} \left(\frac{U_0^2}{v} \frac{\partial U}{\partial z} \right) \frac{\partial z}{\partial z^*} = \frac{U_0^3}{v^2} \frac{\partial^2 U}{\partial z^2} \quad (4.33)$$

$$\frac{\partial V^*}{\partial z^{*2}} = \frac{\partial}{\partial z} \left(\frac{U_0^2}{v} \frac{\partial V}{\partial z} \right) \frac{\partial z}{\partial z^*} = \frac{U_0^3}{v^2} \frac{\partial^2 V}{\partial z^2} \quad (4.34)$$

$$\frac{\partial T^*}{\partial y^*} = \frac{\partial T^*}{\partial \theta} \frac{\partial \theta}{\partial y} \frac{\partial y}{\partial y^*} = (T_w^* - T_\infty^*) \frac{U_0}{v} \frac{\partial \theta}{\partial y} \quad (4.35)$$

$$\frac{\partial^2 T^*}{\partial z^{*2}} = \frac{\partial}{\partial z} \left(\frac{U_0(T_w^* - T_\infty^*)}{v} \frac{\partial \theta}{\partial z} \right) \frac{\partial z}{\partial z^*} = U_0^2 \frac{(T_w^* - T_\infty^*)}{v^2} \frac{\partial^2 \theta}{\partial z^2} \quad (4.36)$$

When the above scaling variables are used and substituted into (4.24) gives;

$$\frac{U_0^3}{v} \frac{\partial U}{\partial t} + \frac{U_0^3}{v} V \frac{\partial U}{\partial y} = \frac{U_0^3}{v} \left(\frac{\partial^2 U}{\partial z^2} \right) - \frac{\partial \bar{u}\bar{w}}{\partial z} - g\beta(T_w^* - T_\infty^*) + \frac{\sigma\mu_e^2 H_0^2 (mV^* - U^*)}{1 + m^2}, \quad (4.37)$$

Thus

$$\frac{U_0^3}{v} \frac{\partial U}{\partial t} + \frac{U_0^3}{v} V \frac{\partial U}{\partial y} = \frac{U_0^3}{v} \left(\frac{\partial^2 U}{\partial z^2} \right) - \frac{\partial \bar{u}\bar{w}}{\partial z} - g\beta(T_w^* - T_\infty^*) + \frac{\sigma\mu_e^2 H_0^2 U_0 (mV - U)}{1 + m^2} \quad (4.38)$$

Equation (4.37) when rearranged gives

$$\frac{\partial U}{\partial t} + V \frac{\partial U}{\partial y} = \left(\frac{\partial^2 U}{\partial z^2} \right) - \frac{\partial \bar{u}\bar{w}}{\partial z} - \frac{\nu g \beta (T_w^* - T_\infty^*)}{U_0^3} + \frac{\sigma \mu_e^2 H_0^2 \gamma (mV - U)}{U_0^2 (1 + m^2)} \quad (4.39)$$

Considering the non-dimensional parameters given as

$$Gr = \frac{\nu g \beta (T_w^* - T_\infty^*)}{U_0^3},$$

$$\theta = \frac{T^* - T_w^*}{T_w^* - T_\infty^*},$$

$$M^2 = \frac{\sigma \mu_e^2 H_0^2 \nu}{U_0^2},$$

Equation (4.38) yields,

$$\frac{\partial U}{\partial t} + V \frac{\partial U}{\partial y} = \left(\frac{\partial^2 U}{\partial z^2} \right) - \frac{\partial \bar{u}\bar{w}}{\partial z} - Gr\theta + \frac{M^2(mV - U)}{(1 + m^2)} \quad (4.40)$$

Following the same procedure, it can also be shown that equation (4.25) results in;

$$\frac{U_0^3}{v} \frac{\partial V}{\partial t} + \frac{U_0^3}{v} V \frac{\partial V}{\partial y} = \frac{U_0^3}{v^2} \left(\frac{\partial^2 V}{\partial z^2} \right) - \frac{\partial \bar{v}\bar{w}}{\partial z} - \frac{\sigma \mu_e^2 H_0^2 U_0 (mU + V)}{1 + m^2} \quad (4.41)$$

On rearranging equation (4.41) gives

$$\frac{\partial V}{\partial t} + V \frac{\partial V}{\partial y} = \frac{1}{v} \left(\frac{\partial^2 V}{\partial z^2} \right) - \frac{\partial \bar{v}\bar{w}}{\partial z} - \frac{\sigma \mu_e^2 H_0^2 U_0 (mU + V)}{1 + m^2} \quad (4.42)$$

Introducing non-dimensional parameters equation (4.42) reduces to;

$$\frac{\partial V}{\partial t} + V \frac{\partial V}{\partial y} = \left(\frac{\partial^2 V}{\partial z^2} \right) - \frac{\partial \bar{v}\bar{w}}{\partial z} - \frac{M^2(mU + V)}{1 + m^2} \quad (4.43)$$

$$\text{Where } M^2 = \frac{\sigma \mu_e^2 H_0^2 \nu}{U_0^2}$$

Considering equation (4.3) and substituting (4.31), (4.35) and (4.36) into it yields

$$(T_w^* - T_\infty^*) \frac{U_0^2}{v} \frac{\partial \theta}{\partial t} + (T_w^* - T_\infty^*) \frac{U_0^2}{v} V \frac{\partial \theta}{\partial y} = \frac{k U_0^2 (T_w^* - T_\infty^*)}{\rho C_p v^2} \frac{\partial^2 \theta}{\partial z^2} - \frac{\partial \bar{wT}}{\partial z} \quad (4.44)$$

Rearranging equation (4.44) yields,

$$\frac{\partial \theta}{\partial t} + V \frac{\partial \theta}{\partial y} = \frac{k}{\rho C_p v} \left(\frac{\partial^2 \theta}{\partial z^2} \right) - \frac{\partial \bar{wT}}{\partial z} \quad (4.45)$$

Using the non-dimensional parameter $Pr = \frac{\mu C_p}{k}$

Equation 4.45 reduces to

$$Pr \left(\frac{\partial \theta}{\partial t} + V \frac{\partial \theta}{\partial y} \right) = \left(\frac{\partial^2 \theta}{\partial z^2} \right) - Pr \frac{\partial \bar{wT}}{\partial z} \quad (4.46)$$

Thus the governing equations are as follows:

$$\frac{\partial U}{\partial t} + V \frac{\partial U}{\partial y} = \left(\frac{\partial^2 U}{\partial z^2} \right) - \frac{\partial \bar{uw}}{\partial z} - Gr\theta + \frac{M^2(mV-U)}{(1+m^2)} \quad (4.47)$$

$$\frac{\partial V}{\partial t} + V \frac{\partial V}{\partial y} = \left(\frac{\partial^2 V}{\partial z^2} \right) - \frac{\partial \bar{vw}}{\partial z} - \frac{M^2(mU+V)}{1+m^2} \quad (4.48)$$

$$Pr \left(\frac{\partial \theta}{\partial t} + V \frac{\partial \theta}{\partial y} \right) = \left(\frac{\partial^2 \theta}{\partial z^2} \right) - Pr \frac{\partial \bar{wT}}{\partial z} \quad (4.49)$$

Boundary and initial conditions are,

$$t < 0, U = 0, V = 0, \theta = 0, \text{ everywhere}$$

$$t \geq 0, U = 0, V = 0, \theta = 0, \text{ at } z \rightarrow \infty$$

$$U = 1, V = 0, \theta = 1, \text{ at } z = 0$$

4.4 Prandtl Mixing Length Hypothesis

It is not possible to solve these equations due to the existence of the Reynolds stresses $\overline{u'v'}$, $\overline{v'w'}$ and $\overline{w'T}$ in equations (4.47) and (4.48) and (4.49) respectively. Therefore the need to adopt the Boussinesque approximation given as:

$$\tau_t = -\rho\overline{u'v'} = A_\tau \frac{dU}{dy} \quad (4.50)$$

It is worth noting that A_τ is not a fluid property as μ but depends on mean velocity U . On the other hand, $\rho\overline{u'v'}$ stands for flux of x- momentum in the y-direction, which is assumed that this momentum was transported by eddies which moved in the y-direction over a given distance say l with no interaction and then mixed with the existing fluid at the new location i.e momentum is taken to be conserved over distance l , (McComb, 1992).

Prandtl was able to deduce experimentally that:

$$\rho\overline{u'v'} = -\rho l^2 \left(\frac{\partial U}{\partial y} \right)^2 \quad (4.51)$$

At this stage, more assumptions are taken as follows:

- i) $y > 5$, viscous term in shear stress is neglected.
- ii) $l = ky$, where k is the karman constant given as $k = 0.4$, McComb, (1992).

On substituting l^2 , it yields:

$$\rho\overline{u'v'} = \rho k^2 y^2 \left(\frac{\partial U}{\partial y} \right)^2 \text{ This reduces to}$$

$$\overline{u'v'} = -k^2 y^2 \left(\frac{\partial U}{\partial y} \right)^2 \quad (4.52)$$

From equation (4.52) can be deduced further to give

$$\overline{uw} = -k^2 z^2 \left(\frac{\partial U}{\partial z} \right)^2 \quad (4.53)$$

And,

$$\overline{vw} = -k^2 z^2 \left(\frac{\partial V}{\partial z} \right)^2 \quad (4.54)$$

Considering the turbulent Prandtl number also given by

$$Pr_t = \frac{\varepsilon_M}{\varepsilon_H} \quad \text{where } \varepsilon_M = -2k^2 z^2 \frac{\partial \bar{u}}{\partial z}$$

Thus,

$$\text{It can be deduced from (4.52) that } \overline{WT} = \frac{-2k^2 z^2 \frac{\partial \bar{u}}{\partial z} \frac{\partial \theta}{\partial z}}{\varepsilon_M} \quad (4.55)$$

Substituting equations (4.52), (4.53), (4.54) and (4.55) to (4.47), (4.48) and (4.49) yield the following set of differential equations as:

$$\frac{\partial U}{\partial t} + V \frac{\partial U}{\partial y} = \left(\frac{\partial^2 U}{\partial z^2} \right) + \frac{\partial}{\partial z} \left[k^2 z^2 \left(\frac{\partial U}{\partial z} \right)^2 \right] + Gr\theta + \frac{M^2(mU+V)}{(1+m^2)} \quad (4.56)$$

$$\frac{\partial V}{\partial t} + V \frac{\partial V}{\partial x} = \left(\frac{\partial^2 V}{\partial z^2} \right) - \frac{\partial}{\partial z} \left[k^2 z^2 \left(\frac{\partial U}{\partial z} \right)^2 \right] - \frac{M^2(mV-U)}{1+m^2} \quad (4.57)$$

$$Pr \left(\frac{\partial \theta}{\partial t} + V \frac{\partial \theta}{\partial y} \right) = \left(\frac{\partial^2 \theta}{\partial z^2} \right) + Pr \left(\frac{2k^2 z^2 \frac{\partial \bar{u}}{\partial z} \frac{\partial \theta}{\partial z}}{Pr_t} \right) \quad (4.58)$$

Equations (4.56) and (4.57) can be simplified further and then the final set of the governing equations given as:

$$\frac{\partial U}{\partial t} + V \frac{\partial U}{\partial y} = \left(\frac{\partial^2 U}{\partial z^2} \right) + 2k^2 z \left(\frac{\partial U}{\partial z} \right)^2 + 2k^2 z^2 \left(\frac{\partial^2 U}{\partial z^2} \right) \left(\frac{\partial U}{\partial z} \right) + Gr\theta + \frac{M^2(mU+V)}{(1+m^2)} \quad (4.59)$$

$$\frac{\partial V}{\partial t} + V \frac{\partial V}{\partial y} = \left(\frac{\partial^2 V}{\partial z^2} \right) + 2k^2 z \left(\frac{\partial V}{\partial z} \right)^2 + 2k^2 z^2 \left(\frac{\partial^2 V}{\partial z^2} \right) \left(\frac{\partial V}{\partial z} \right) - \frac{M^2(mV-U)}{1+m^2} \quad (4.60)$$

$$Pr \left(\frac{\partial \theta}{\partial t} + V \frac{\partial \theta}{\partial y} \right) = \left(\frac{\partial^2 \theta}{\partial z^2} \right) + Pr \left(\frac{2k^2 z^2}{Pr_t} \frac{\partial \bar{u}}{\partial z} \frac{\partial \theta}{\partial z} \right) \quad (4.61)$$

Equations (4.59), (4.60) and (4.61) represent the final set of the governing equations. The next step is the determination of the numerical solution to these governing equations subject to the initial and boundary conditions given below.

4.5 Boundary And Initial Conditions

$t < 0$, $U = 0$, $V = 0$, $\theta = 0$, everywhere

$t \geq 0$, $U = 0$, $V = 0$, $\theta = 0$, at $z \rightarrow \infty$

$U = 1$, $V = 0$, $\theta = 1$, at $z = 0$

4.6. Explicit Finite Difference Scheme

The explicit finite difference scheme is employed in the solution of these governing equations (4.59), (4.60) and (4.61) since they are highly non-linear. The mesh shown in *figure 3.1* and the equivalent Finite difference Scheme for these governing equations are respectively given as:

$$\begin{aligned} \frac{U_{(i,j+1)} - U_{(i,j)}}{\Delta t} + V_{(i,j)} \frac{U_{(i+1,j)} - U_{(i,j)}}{\Delta y} &= \left(\frac{U_{(i+1,j)} - 2U_{(i,j)} + U_{(i-1,j)}}{(\Delta z)^2} \right) + 0.32i\Delta z \left(\frac{U_{(i+1,j)} - U_{(i,j)}}{\Delta z} \right)^2 + \\ 0.32(i\Delta z)^2 \left(\frac{U_{(i+1,j)} - 2U_{(i,j)} + U_{(i-1,j)}}{(\Delta z)^2} \right) \left(\frac{U_{(i+1,j)} - U_{(i,j)}}{\Delta z} \right) &+ Gr\theta_{i,j} + M^2 \left(\frac{mV_{(i,j)} - U_{(i,j)}}{1+m^2} \right) \end{aligned} \quad (4.62)$$

$$\begin{aligned} \frac{V_{(i,j+1)} - V_{(i,j)}}{\Delta t} + V_{(i,j)} \frac{V_{(i+1,j)} - V_{(i,j)}}{\Delta y} &= \left(\frac{V_{(i+1,j)} - 2V_{(i,j)} + V_{(i-1,j)}}{(\Delta z)^2} \right) + 0.32i\Delta z \left(\frac{V_{(i+1,j)} - V_{(i,j)}}{\Delta z} \right)^2 + \\ 0.32(i\Delta z)^2 \left(\frac{V_{(i+1,j)} - 2V_{(i,j)} + V_{(i-1,j)}}{(\Delta z)^2} \right) \left(\frac{V_{(i+1,j)} - V_{(i,j)}}{\Delta z} \right) &+ Gr\theta_{i,j} + M^2 \left(\frac{mU_{(i,j)} + V_{(i,j)}}{1+m^2} \right) \end{aligned} \quad (4.63)$$

$$\begin{aligned} Pr \left(\frac{\theta_{(i,j+1)} - \theta_{(i,j)}}{\Delta t} + V_{i,j} \frac{\theta_{i+1,j} - \theta_{i,j}}{\Delta y} \right) &= \left(\frac{\theta_{(i+1,j)} - 2\theta_{(i,j)} + \theta_{(i-1,j)}}{\Delta z^2} \right) + \\ 0.32(i\Delta z)^2 \frac{Pr}{Pr_t} \left\{ \left(\frac{U_{(i+1,j)} - U_{(i,j)}}{\Delta z} \right) \left(\frac{\theta_{(i+1,j)} - \theta_{(i,j)}}{\Delta z} \right) \right\} & \end{aligned} \quad (4.64)$$

In this case, $k = 0.4$, $z = i\Delta z$ and i and j refer to z and t respectively.

The initial and boundary conditions will now take the form given as:

$$U_{i,j} = 0; V_{i,j} = 0; \theta_{i,j} = 0 \text{ Everywhere for } j < 0$$

$$j \geq 0; U_{i,j} = 0; V_{i,j} = 0; \theta_{i,j} = 0 \text{ For } i = \infty \quad (4.65)$$

$$U_{i,j} = 1; V_{i,j} = 0; \theta_{i,j} = 1 \text{ For } i = 0$$

The computation for the consecutive grid points for primary and secondary velocities and temperature can now be done using the initial and boundary conditions (4.65), that is $U_{(i,j+1)}$,

$V_{(i,j+1)}$ and $\theta_{(i,j+1)}$.

$$\begin{aligned} U_{(i,j+1)} &= U_{(i,j)} + \Delta t \left\{ -V_{(i,j)} \frac{U_{(i+1,j)} - U_{(i,j)}}{\Delta y} + \left(\frac{U_{(i+1,j)} - 2U_{(i,j)} + U_{(i-1,j)}}{(\Delta z)^2} \right) + \right. \\ 0.32i\Delta z \left(\frac{U_{(i+1,j)} - U_{(i,j)}}{\Delta z} \right)^2 &+ 0.32(i\Delta z)^2 \left(\frac{U_{(i+1,j)} - 2U_{(i,j)} + U_{(i-1,j)}}{(\Delta z)^2} \right) \left(\frac{U_{(i+1,j)} - U_{(i,j)}}{\Delta z} \right) + Gr\theta_{i,j} + \\ M^2 \left(\frac{mV_{(i,j)} - U_{(i,j)}}{1+m^2} \right) &\left. \right\} \end{aligned} \quad (4.66)$$

$$\begin{aligned}
V_{(i,j+1)} = & V_{(i,j)} + \Delta t \left\{ -V_{(i,j)} \frac{V_{(i+1,j)} - V_{(i,j)}}{\Delta y} + \left(\frac{V_{(i+1,j)} - 2V_{(i,j)} + V_{(i-1,j)}}{(\Delta z)^2} \right) + 0.32 i \Delta z \left(\frac{V_{(i+1,j)} - V_{(i,j)}}{\Delta z} \right)^2 \right. \\
& \left. + 0.32 (i \Delta z)^2 \left(\frac{V_{(i+1,j)} - 2V_{(i,j)} + V_{(i-1,j)}}{(\Delta z)^2} \right) \left(\frac{V_{(i+1,j)} - V_{(i,j)}}{\Delta z} \right) + Gr \theta_{i,j} + M^2 \left(\frac{mU_{(i,j)} + V_{(i,j)}}{1+m^2} \right) \right\} \quad (4.67)
\end{aligned}$$

$$\begin{aligned}
\theta_{i,j+1} = & \theta_{(i,j)} + \Delta t \left\{ -V_{i,j} \frac{\theta_{i+1,j} - \theta_{i,j}}{\Delta y} + \frac{1}{Pr} \left[\left(\frac{\theta_{(i+1,j)} - 2\theta_{(i,j)} + \theta_{(i-1,j)}}{\Delta z^2} \right) + \right. \right. \\
& \left. \left. 0.32 (i \Delta z)^2 \frac{Pr}{Pr_t} \left\{ \left(\frac{U_{(i+1,j)} - U_{(i,j)}}{\Delta z} \right) \left(\frac{\theta_{(i+1,j)} - \theta_{(i,j)}}{\Delta z} \right) \right\} \right] \right\} \quad (4.68)
\end{aligned}$$

4.7 Stability of Explicit Finite Difference Scheme

In order to judge the accuracy of convergence of explicit finite difference scheme, we will consider at least two or more values of Δt , for instance 0.0009, 0.001 and other significant change that may be noticed. If at all instances there is no difference in their values, then the explicit finite difference scheme is stable and convergent.

4.8 Discussion of Results

Graphical presentation of the numerical results of the discretized governing equations from MATLAB is done in this section. Various fluid parameters were varied on primary velocity, U , secondary velocity, V , and temperature, θ , profiles and then discussed. In all these simulations, for both positive and negative Grashof numbers; $Pr_t = 0.85$ and $K = 0.4$, where K is von Karman constant and Pr_t is the turbulent Prandtl number.

4.8.1 Cooling of the Plate

In this case the fluid flow is at alower temperature than the plate itself. This is implied by the positive Grashof number ($Gr > 0$), therefore the plate loose heat to the surrounding.

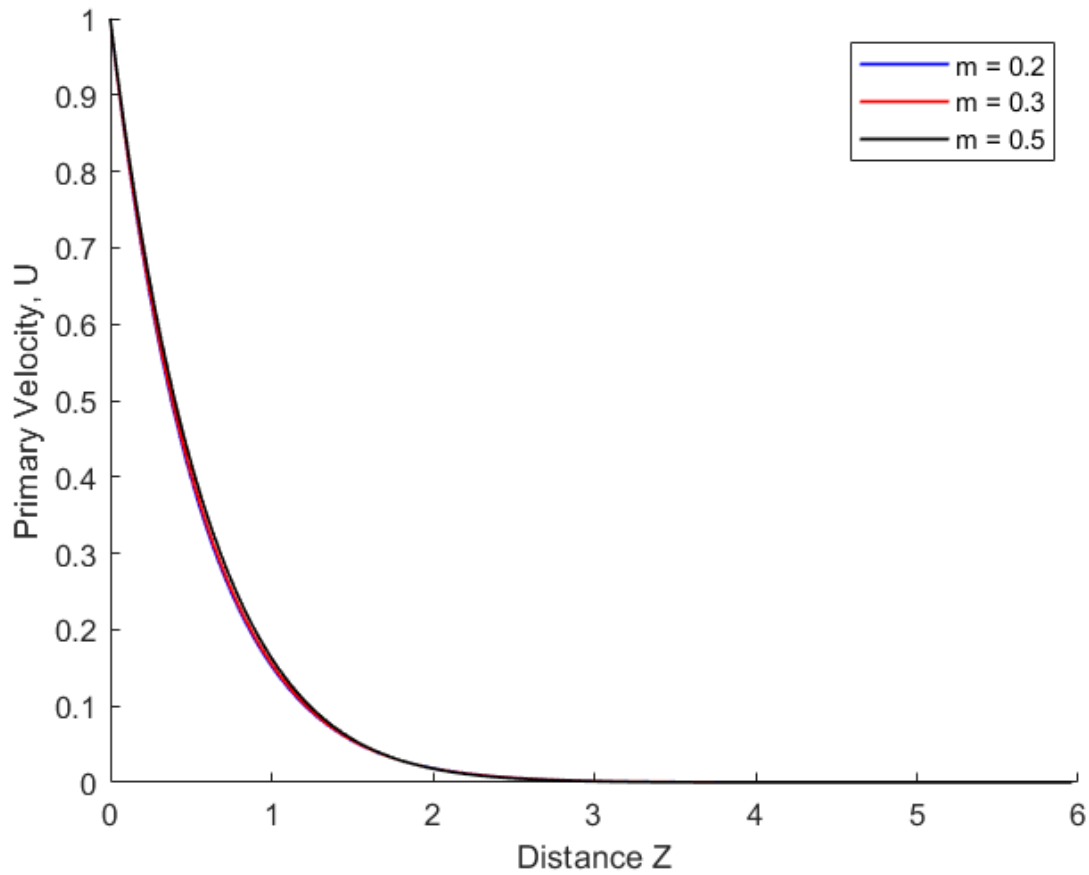


Figure 4.2: Primary velocity profile for Hall current

From this figure, it can be shown that Hall current has little significance to primary velocity.

However, primary velocity decreases with decrease in Hall parameter. This may be attributed to the fact that for a small value of m , the term $\frac{1}{1+m}$ will in turn increase the resistive force of the applied magnetic parameter thus reducing the primary velocity.

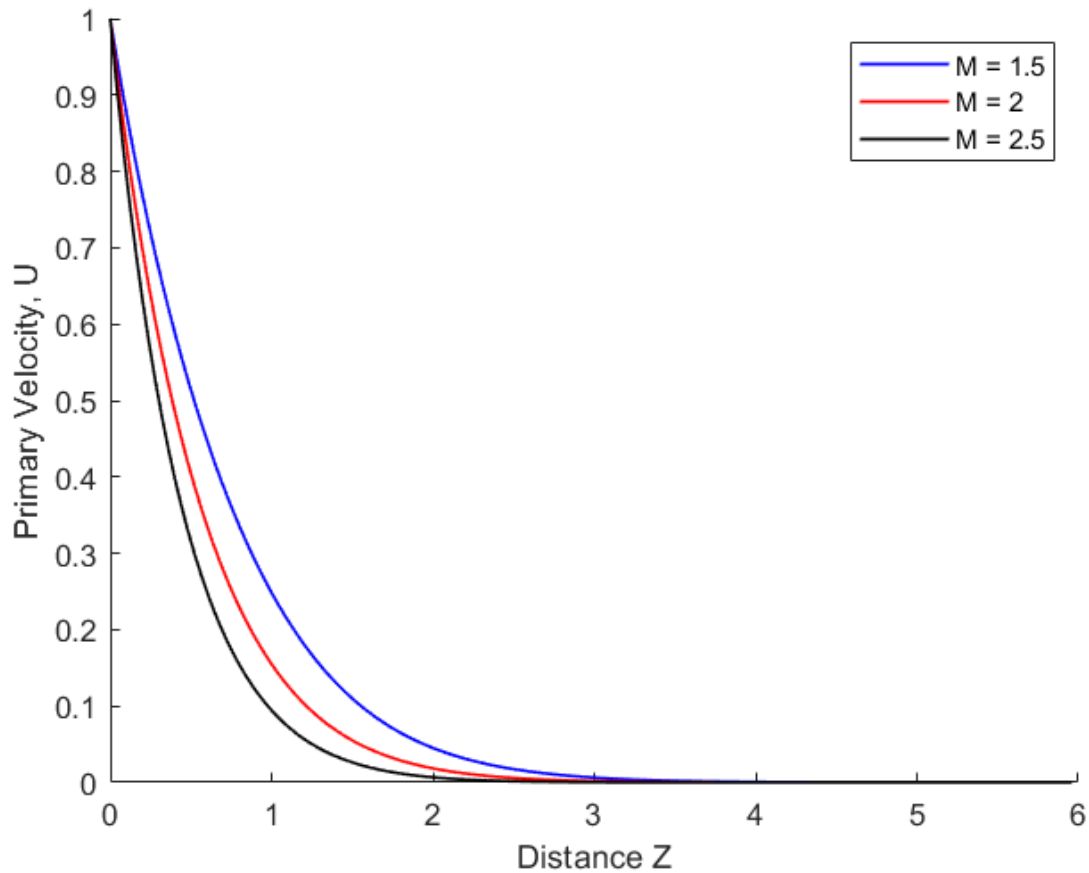


Figure 4.3: Primary velocity profile for Magnetic parameter

Figure 4.3 clearly shows that primary velocity decreases with increase in magnetic parameter. Magnetic parameter, M , refers to the ratio of the magnetic force to inertial force therefore higher M means higher magnetic force acting perpendicularly on an electrically conducting fluid hence developing Lorentz force which is an opposing force to fluid motion thus decreasing the primary velocity.

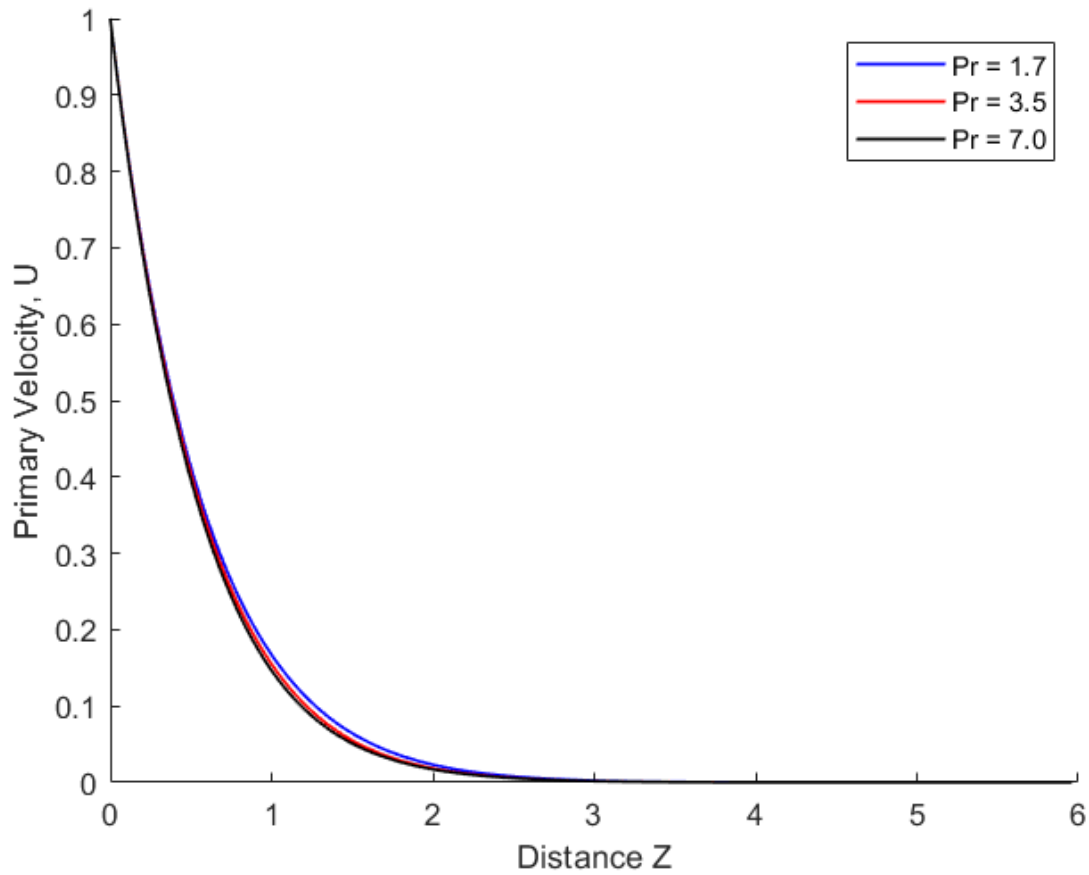


Figure 4.4: Primary velocity profile for Prandtl number

Considering figure 4.4, primary velocity decreases with increase in Prandtl number, Pr , though in a smaller extent. This is because increased Prandtl number leads to increase in viscosity making the fluid more thick thus leading to a decrease in primary velocity.

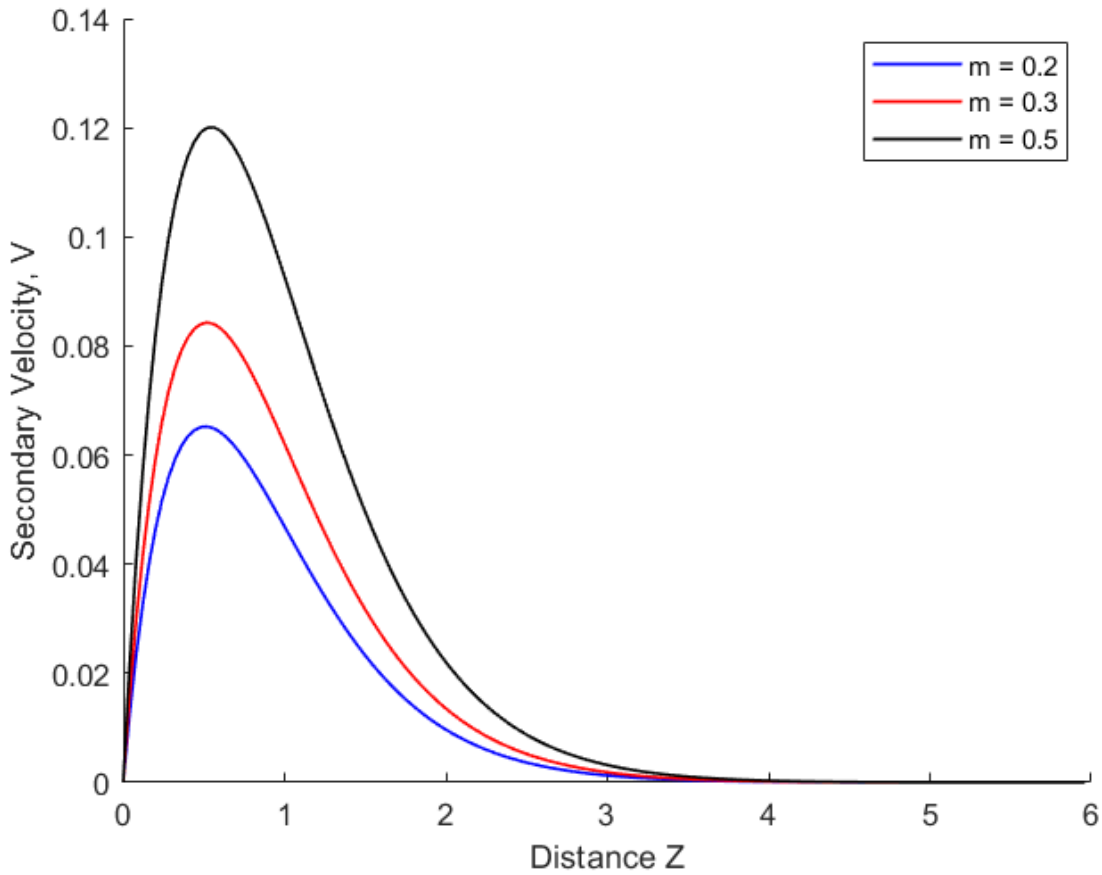


Figure 4.5: Secondary velocity profile for Hall parameter

Figure 4.5 shows a significant decrease in secondary velocity with decrease in Hall parameter, m .

Considering the model equation, and the fact that for any value of m , in the term $\frac{1}{1+m^2}$ will decrease the negative value of M^2 which will in turn decrease the secondary velocity. The decrease in the negative value of M^2 means an increase in magnetic force in an electrically conducting fluid thus developing Lorentz force which opposes fluid motion.

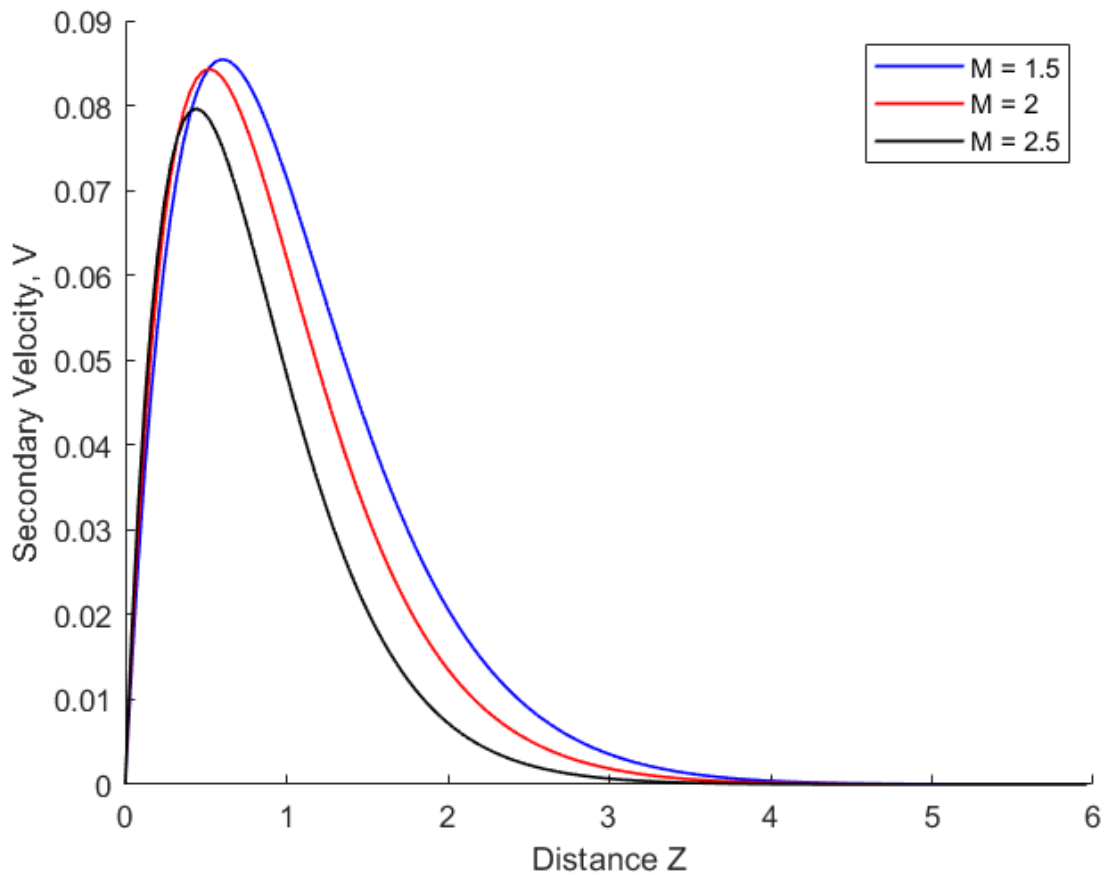


Figure 4.6: Secondary velocity profile for magnetic parameter

From figure 4.6, it is observed that secondary velocity was increased first at the beginning but later was decrease with an increase in magnetic parameter, M . This is because at the beginning, Lorentz force decelerated the primary velocity but increased the lateral flow which in this case is the secondary velocity. The secondary velocity later decreased with increase in magnetic parameter because of the reduction of the magnetic force by the Hall current.

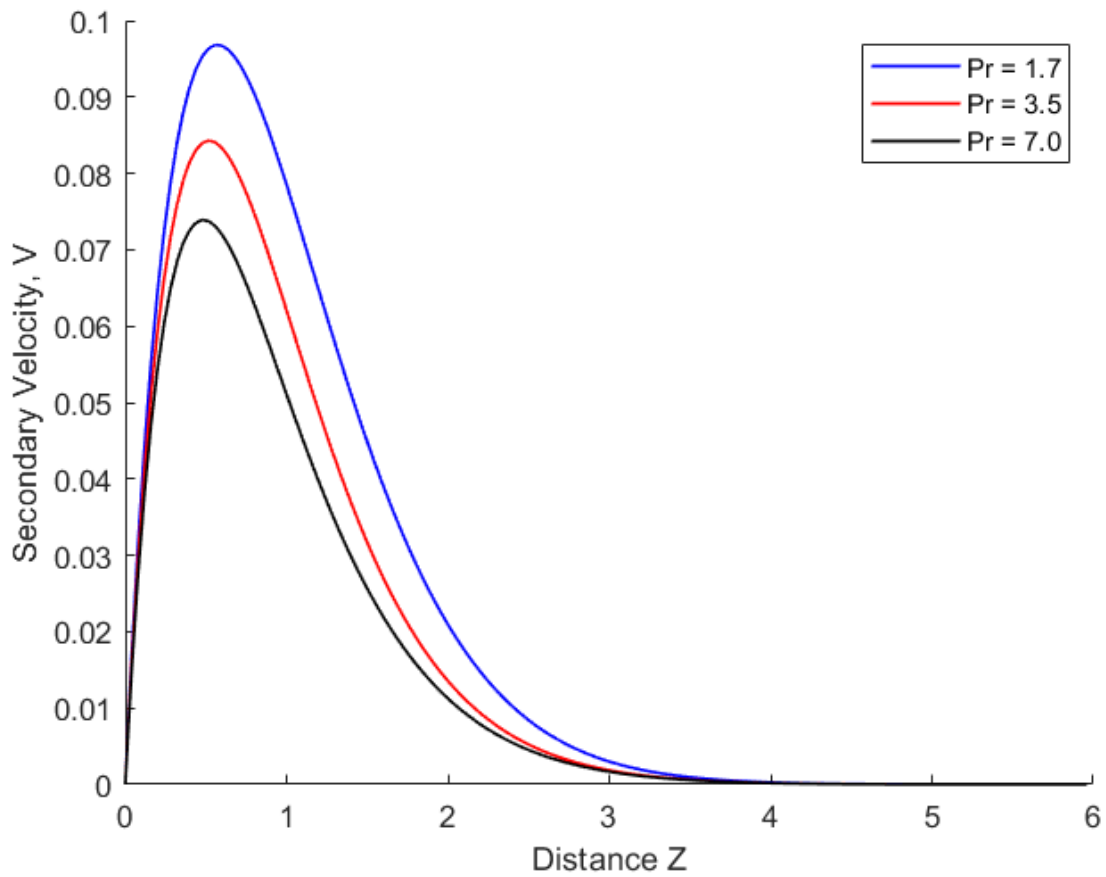


Figure 4.7: Secondary velocity profile for prandtl number

Clearly, figure 4.7 depicts a decrease in secondary velocity with an increase in Prandtl number.

This is due to increased viscosity of the fluid hence decreasing the secondary velocity.

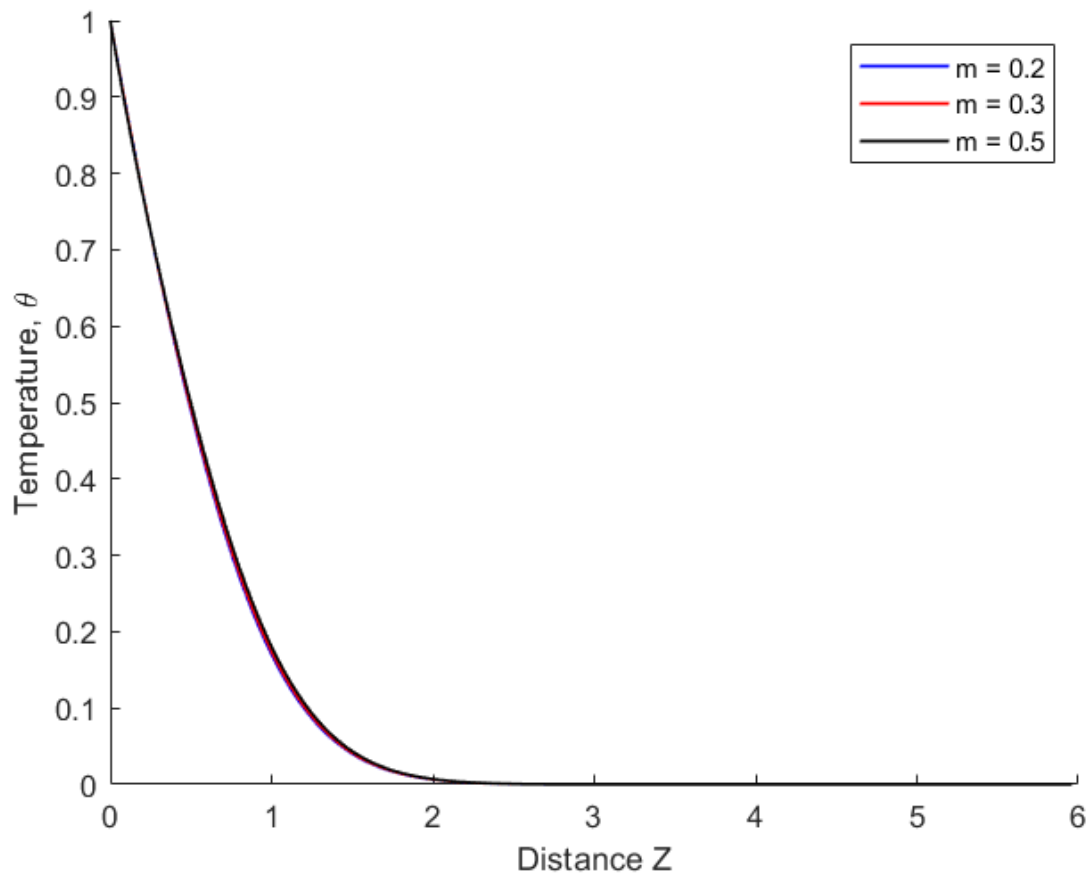


Figure 4.8: Temperature profile for Hall parameter

Figure 4.8 clearly shows that there is no significant change in temperature as the Hall parameter is varied. However, the small change shows that the temperature, θ , of the fluid flow decreases with decrease in Hall parameter.

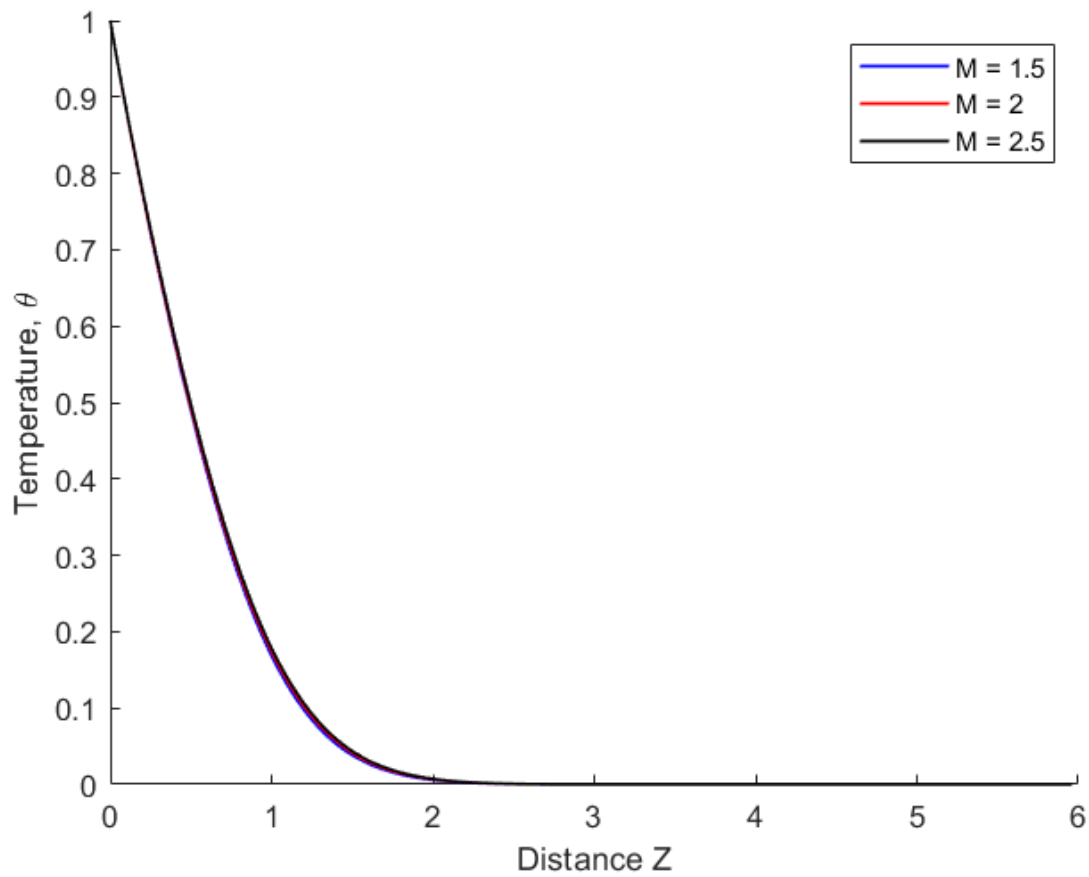


Figure 4.9: Temperature profile for magnetic parameter

From figure 4.9, it shows there is no significant temperature change with variation in magnetic parameter. However, the small change indicates that there is a decrease in temperature profile with increase in magnetic parameter.

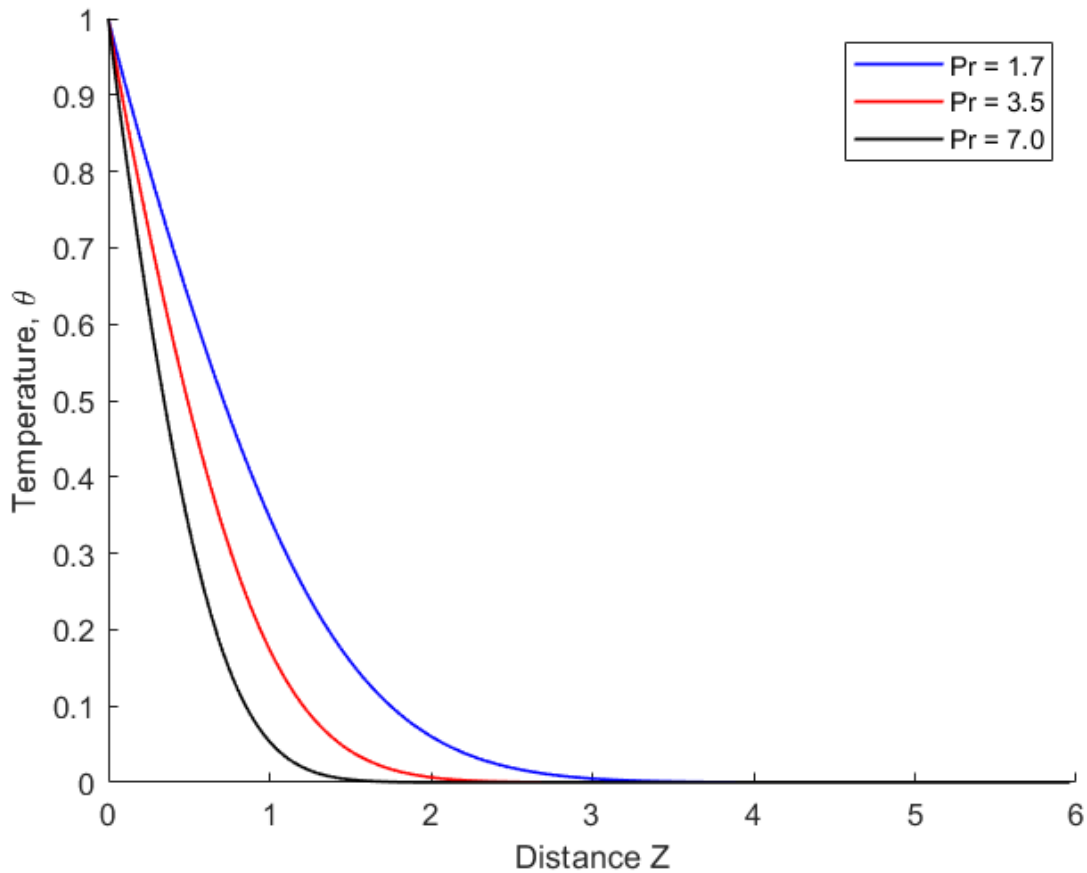


Figure 4.10: Temperature profile for Prandtl number

Figure 4.10 shows that there is a decrease in temperature profile with an increase in prandtl number . since prandtl number is the ratio of momentum diffusivity to thermal diffusivity, thus increased prandtl number means lower thermal diffusivity in comparison to momentum diffusivity hence decreasing thermal boundary layer which will in turn decreases the temperature distribution of the fluid.

4.8.2 Heating of the Plate

The surrounding fluid in this case is at a higher temperature than the plate itself meaning the plate has a lower temperature. This is shown by the negative values of Gr , that is $Gr < 0$.

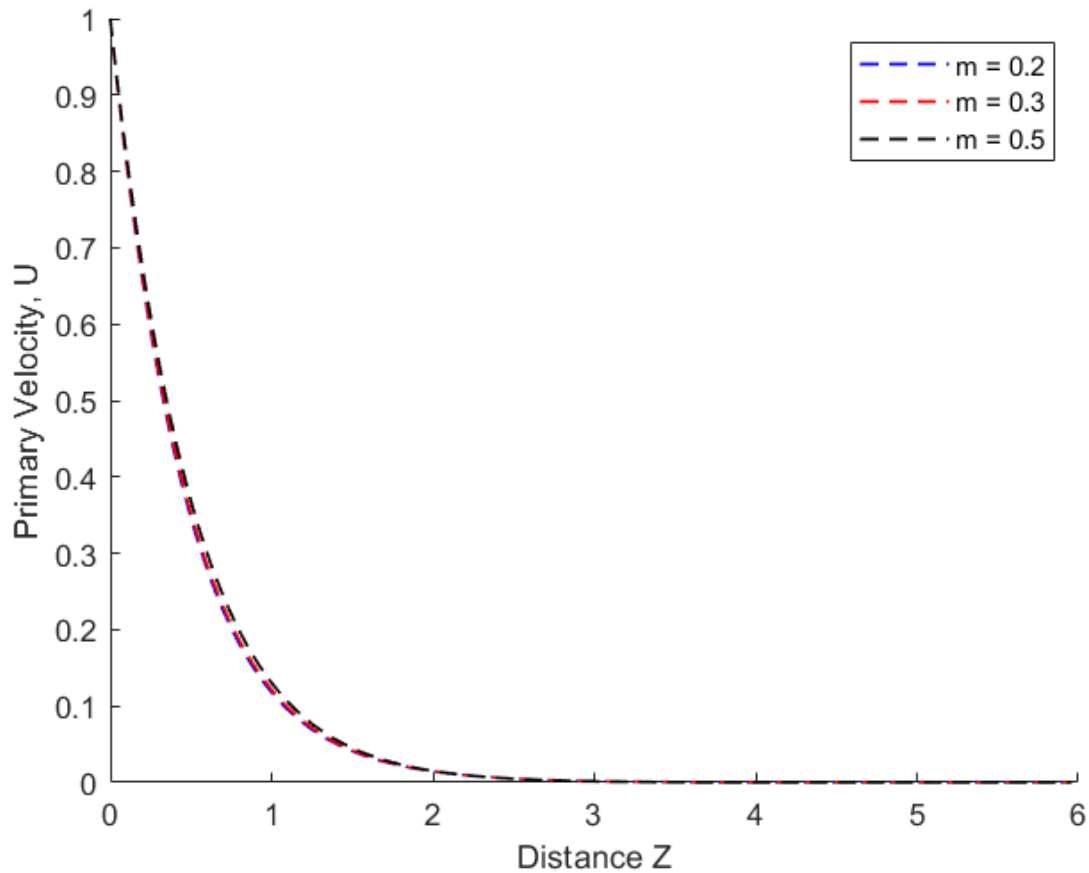


Figure 4.11: Primary velocity profile for Hall parameter

Considering figure 4.11, decrease in Hall parameter leads to a decrease in primary velocity. This is because for a smaller value of m , substituted to the term $\frac{1}{1+m}$ will increase magnetic force which will in turn increases resistive force of the applied magnetic parameter hence decreasing the primary velocity.

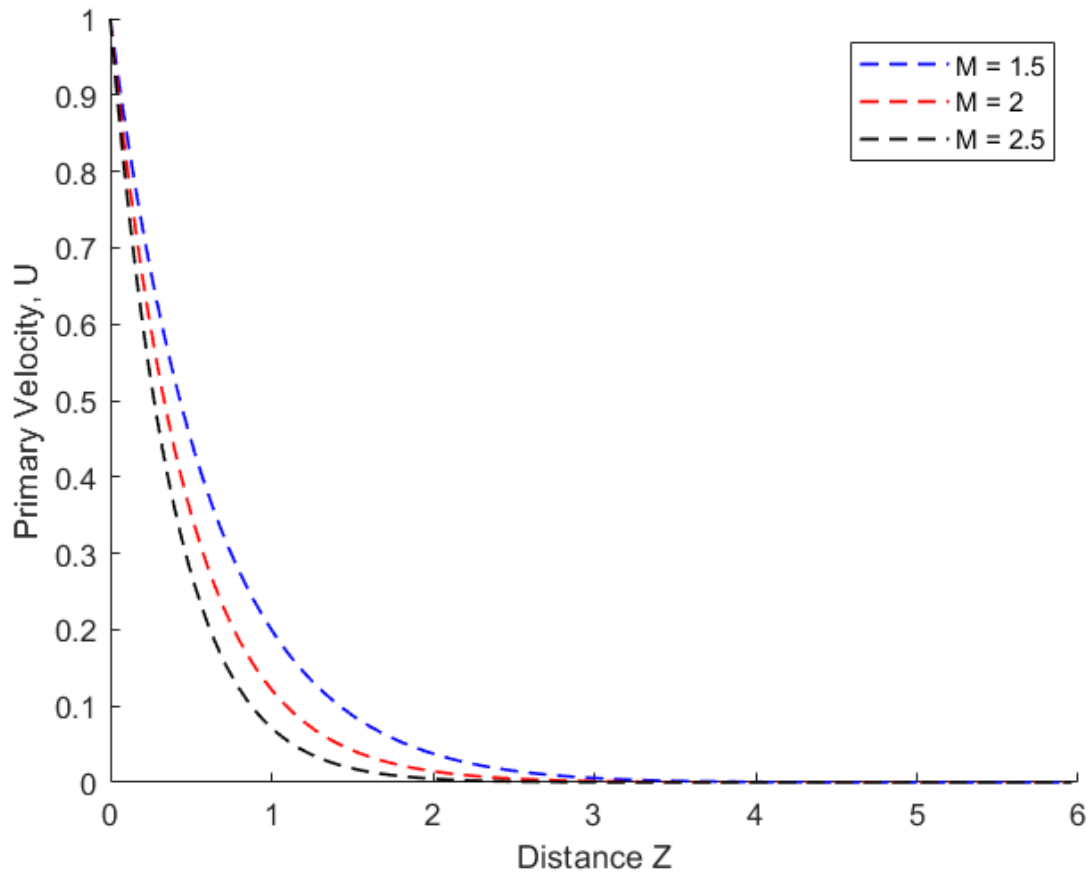


Figure 4.12: Primary velocity profile for Magnetic parameter

With respect to figure 4.12, primary velocity decreases with increase in magnetic parameter. This is attributed to Lorentz force generated by a higher magnitude of the magnetic force acting on an electrically conducting fluid hence decreasing the primary velocity.

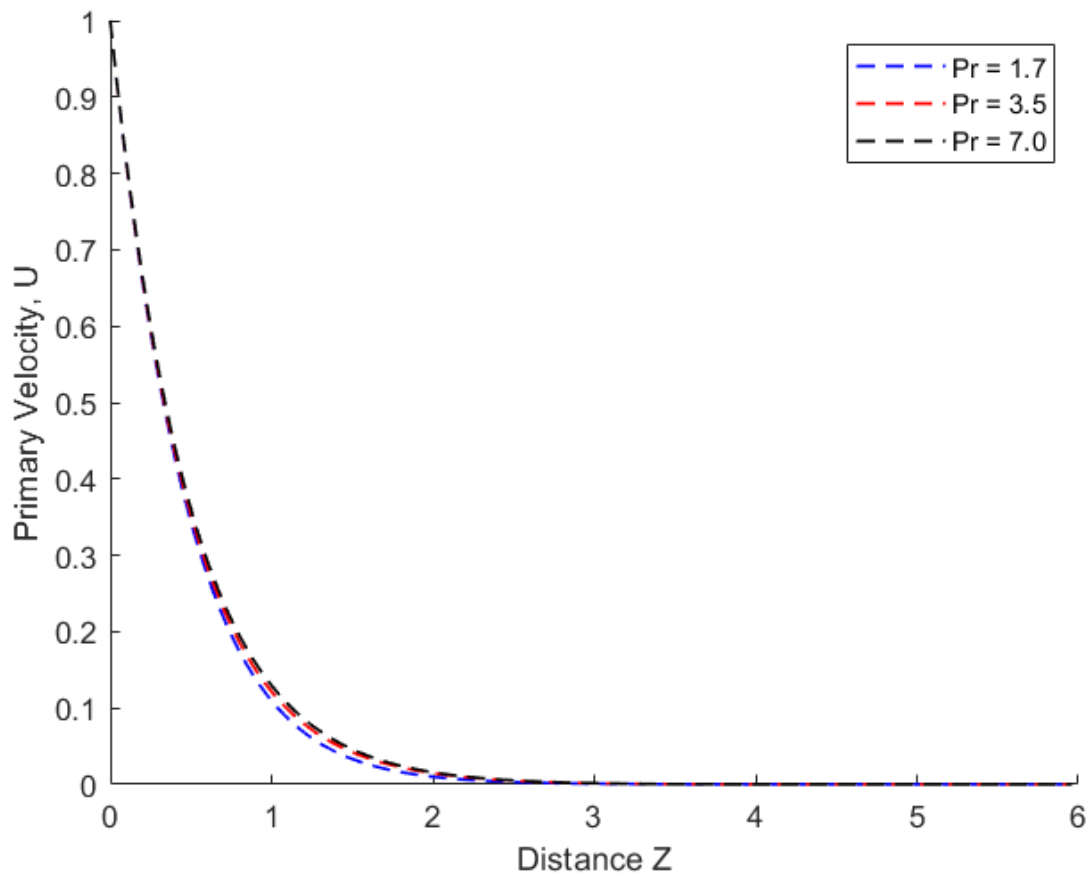


Figure 4.13: Primary velocity profile for Prandtl number

Figure 4.13 indicates that primary velocity decreases with decrease in prandtl number. This is attributed to the fact that prandtl number being a ratio of momentum(product of unit of mass and velocity) to thermal diffusivity , therefore lower prandtl number means thermal diffusivity dominates momentum leading to a decrease in primary velocity.

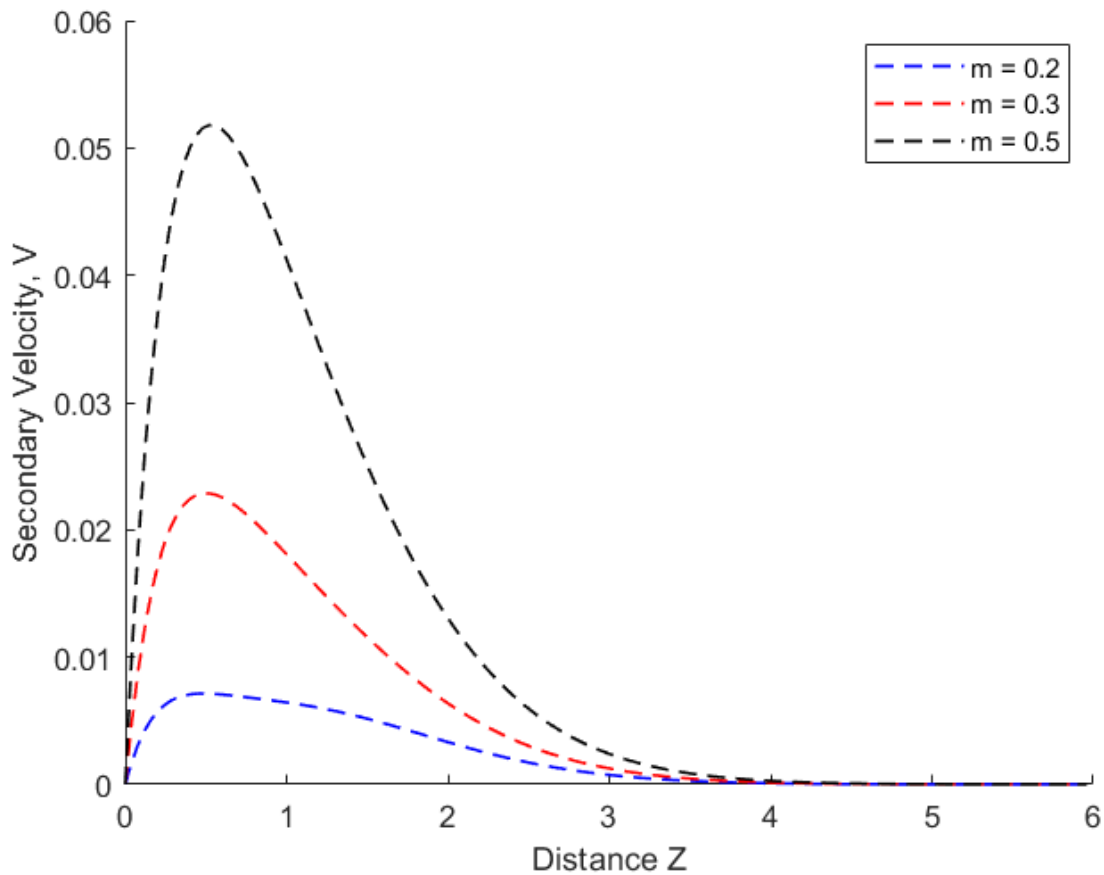


Figure 4.14: Secondary velocity profile for Hall Parameter

Figure 4.14 shows that secondary velocity decreases significantly with a decrease in Hall parameter, m . This is because for a smaller value of m , the term in $\frac{1}{1+m}$ will have a small impact in the value of M^2 as oppose to decreasing magnetic force if there was an increase in m . This will mean that Lorentz force is maintained at a higher value thus decreasing the secondary velocity.

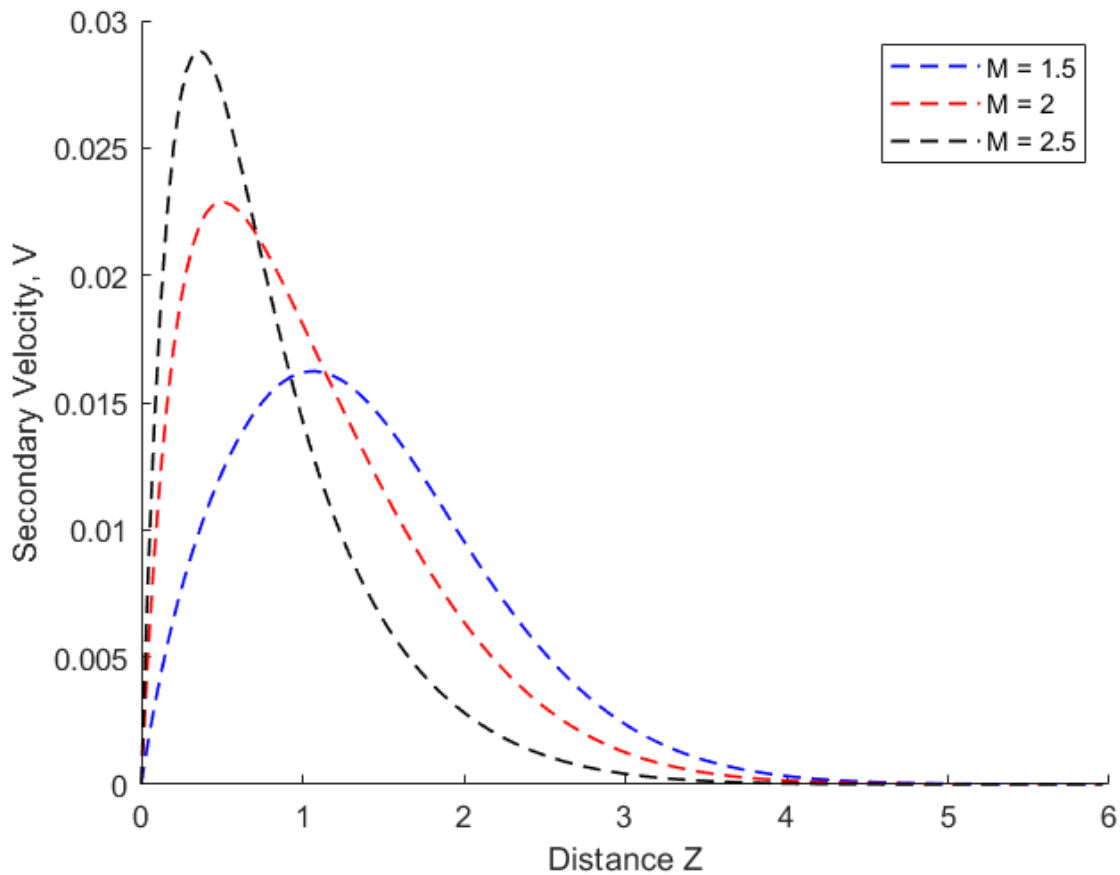


Figure 4.15: Secondary velocity profile for Magnetic parameter

Figure 4.15 illustrates that secondary velocity was accelerated first with increase in magnetic parameter but later decelerated with an increase in magnetic parameter. This is attributed to the fact that increase in magnetic parameter leads to a decrease in primary velocity but increase the lateral flow which is the secondary velocity. However, after some time, the secondary velocity decreased significantly with increase in magnetic parameter because of the reduction of the magnetic force by the Hall parameter.

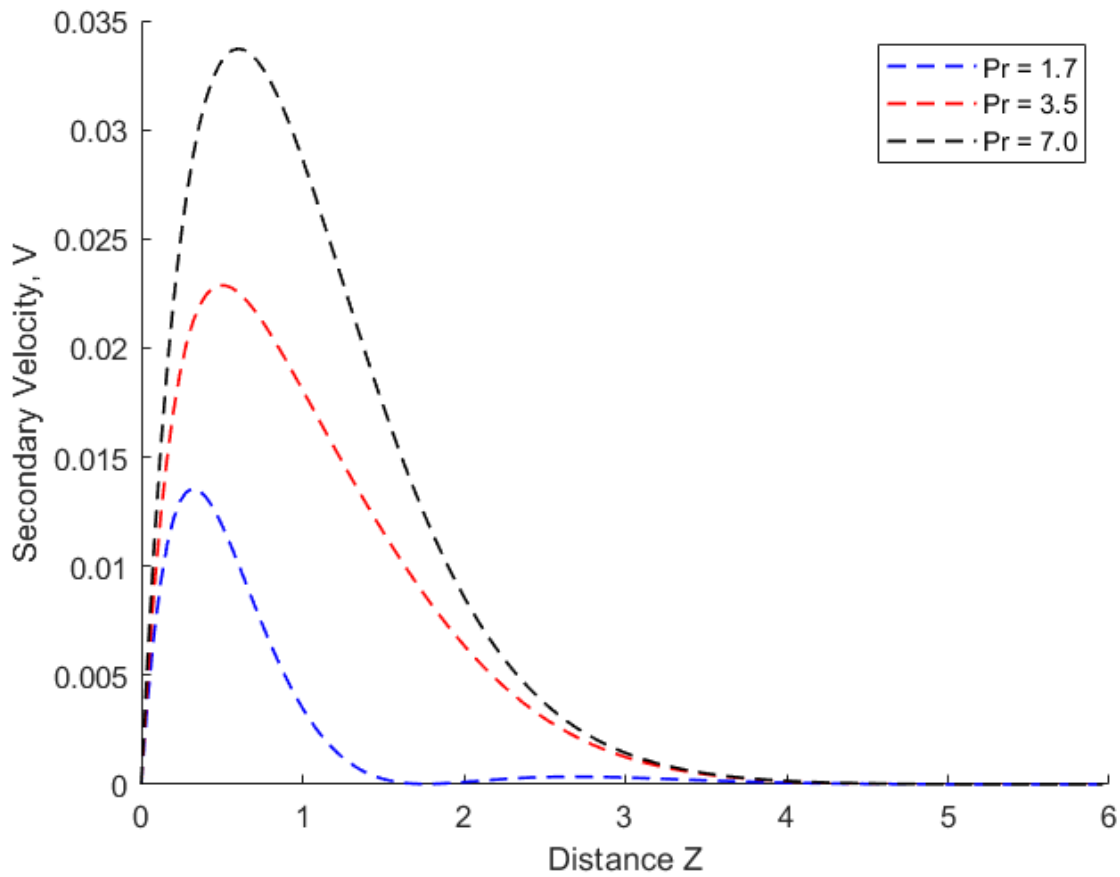


Figure 4.16: Secondary velocity profile for Prandtl number

Secondary velocity decreases with decrease in prandtl number as shown in figure 4.16. This is due to the negative Gr . Decrease in Grashof number implies a decrease in buoyancy force which is responsible for accelerating the fluid motion thus leading to the decrease in secondary velocity.

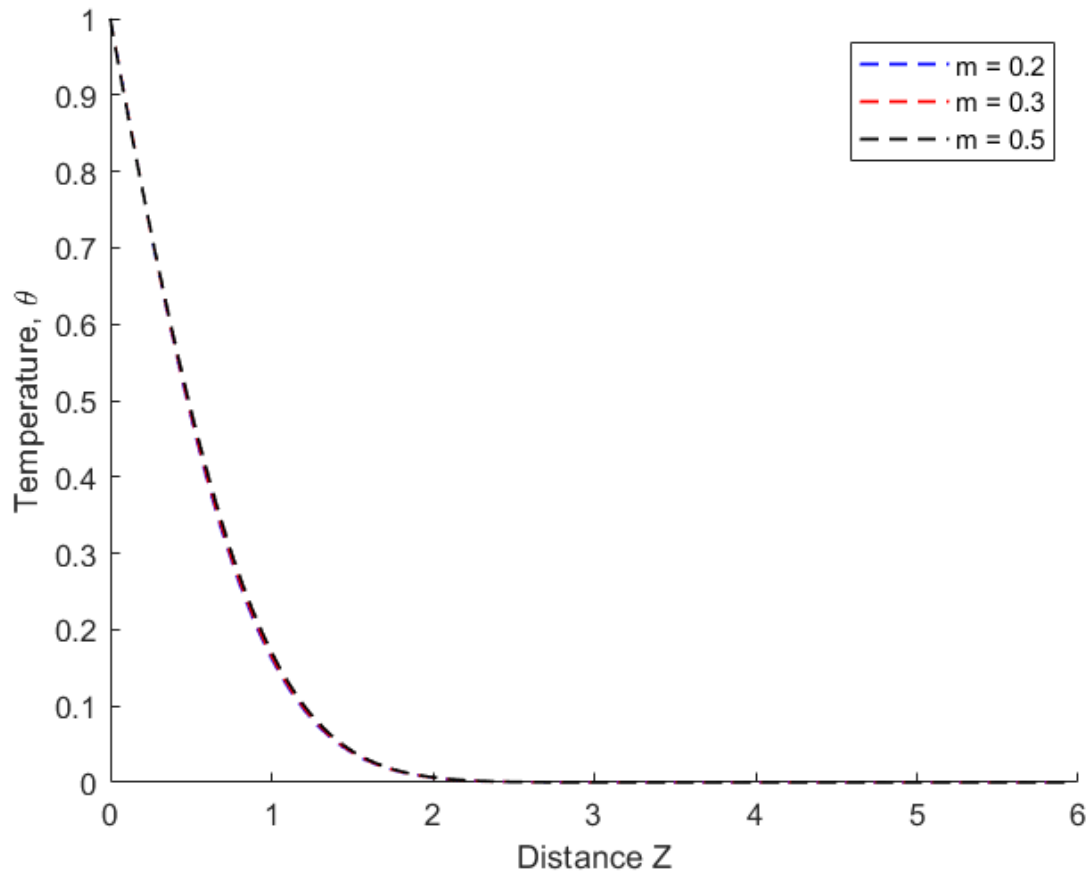


Figure 4.17: Temperature profile for Hall parameter

According to figure 4.17, there is no significance change in temperature when the Hall parameter is decreased. However, there is anepligible decrease in temperature with decrease in Hall parameter.

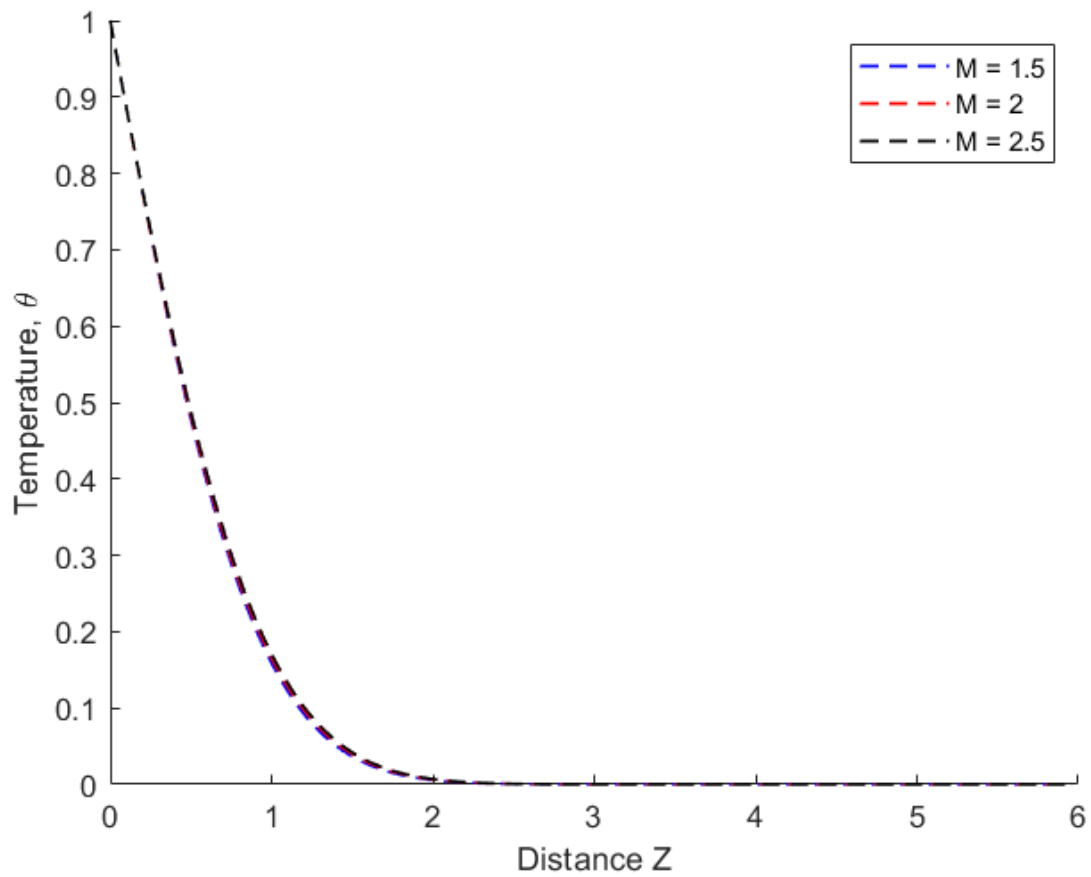


Figure 4.18: Temperature profile for Magnetic parameter

Figure 4.18 shows that there is no significant temperature change when magnetic parameter is decreased.

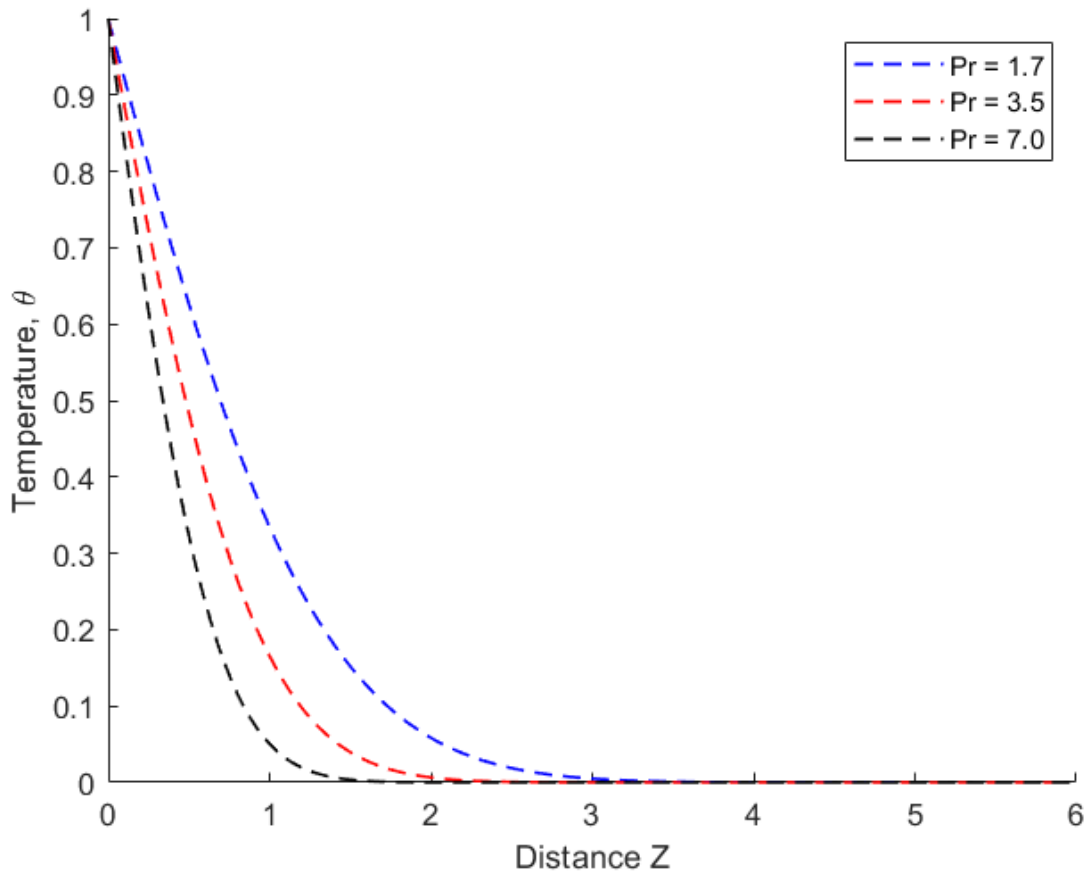


Figure 4.19: Temperature profile Prandtl number

From figure 4.19, it clearly indicates a decrease in temperature profile when Prandtl number is increased. This is attributed to the fact that Pr , being the ratio of momentum diffusivity to thermal diffusivity means there is lower thermal diffusivity in comparison to momentum diffusivity hence decreasing the temperature profile, θ .

4.9 Validation of results

These results when compared with those of Kwanza *et.al* (2010) who developed a mathematical model of turbulent convective fluid flow past an infinite vertical plate with Hall current in a dissipative fluid and found out that an increase in Hall current leads to an increase in velocity profiles. These results are in agreement with the findings of this research. Comparison also with Mukuna *et.al* (2020) who modeled a Hydromagnetic free convection turbulent fluid flow over a vertical infinite plate using turbulent prandtl number. They found out that there is an increase in primary velocity whenever magnetic parameter is decreased, Hall parameter is increased and when Grashof number is increased. It was also evident that secondary velocity increases when magnetic parameter is decreased and decreases when Hall parameter is increased. They also found out that temperature profile decreases when magnetic parameter is decreased, decreases when Hall parameter is increased and also increases when prandtl number decreases. These results also agree with the findings of this research.

CHAPTER FIVE

SUMMARY, CONCLUSIONS AND RECOMMENDATIONS

5.1 Introduction

In this chapter, the summary of the findings are made based on the objectives of the study which is the modeling and analysis of magnetohydrodynamic free convection turbulent fluid flow past an infinite vertical porous plate. Conclusions are made based on the research findings and recommendations are suggested for further research.

5.2 Summary

The study sought to model and analyze magnetohydrodynamic free convection turbulent fluid flow past an infinite vertical porous plate. The Explicit Finite Difference Scheme was used to solve the problem. The developed model proved to be working and the result analysis showed that the findings are in line with the objectives.

5.3 Conclusions

The modeling and analysis of magnetohydrodynamic free convection turbulent fluid flow past an infinite vertical porous plate investigated numerically. The effects of flow parameters like Grashoff numbers, Gr , Prandtl number, Pr , magnetic parameter, M , and Hall parameter, m , on mean primary velocity, U , secondary velocity, V , and temperature profile, θ , obtained. In each case, $P_r_t = 0.85$, and $K = 0.4$. The results are summarized as follows:

- a) A mathematical model that is working developed for a MHD fluid flow using conservation of mass, energy and momentum equations for a flow that is turbulent and past a vertical infinite porous plate.

- b) The partial differential equations associated with the model were numerically solved using the explicit finite difference scheme and the graphical presentations of velocities and temperature profiles given.
- c) The velocities and temperature profiles for various flow parameters were analyzed and it was found that:
- i) During both the cooling and heating of the plate ($Gr > 0$, and $Gr < 0$), the primary velocity decreases with decrease in Hall parameter, m , and increase in magnetic parameter, M . It also decreases during cooling of the plate as the Prandtl number, Pr , is increased and even during the heating of the plate as the Prandtl number, Pr , is decreased.
 - ii) During both the cooling and heating of the plate ($Gr > 0$, and $Gr < 0$), the secondary velocity decreases with decrease in Hall parameter, m , and increase in magnetic parameter, M . It also decreases during cooling of the plate as the Prandtl number, Pr , is increased and also during heating of the plate as the Prandtl number, Pr , is decreased.
 - iii) There is NO significant effect on temperature profile, θ , during both cooling and heating of the plate as the Hall parameter, m , is decreased. There is also NO significant change during the cooling of the plate as the magnetic parameter, M , is increased and even during the heating of the plate as the magnetic parameter, M , is decreased.
- There is decrease in temperature profile when Prandtl number, Pr , is increased in both the cooling and heating of the plate.

5.4 Recommendations

The following recommendations are made based on these findings:

- i) Adoption of the MHD model due to its significance in the field of medicine, engineering and technology as well as security sector. This will inform the progress of development in our society and the country at large.
- ii) The use of explicit finite difference scheme for the solution of PDEs that are highly non-linear because of its level of accuracy since it is stable and convergent.
- iii) The use of flow parameters like Prandtl number, Grashof number, Hall parameter, magnetic parameter and turbulent prandtl number since it is able to analyze the velocities and temperature profiles appropriately.

5.5 Suggestions for further Research

There is still a lot of research that can be done on MHD turbulent fluid flows therefore the following recommendations are made to further the research on this topic:

- a) Fluid flow that is compressible
- b) Considering a cylindrical plate.
- c) Considering magnetic field inclined at an angle.
- d) Using other methods to resolve turbulent stresses other than Prandtl mixing length hypothesis.

REFERENCES

1. Bejan, A. (1995). *Heat Transfer* (2nd ed). New York: Wiley.
2. Begum J.A., Addul Maleque M. D., Ferows M., Mota (2013). Finite Difference solution of Natural Convective flow over a heated plate with different inclination and stability, *Applied mathematical sciences*, 6(66), 3367-3379
3. Chebos C., Sigey J.K, Okelo J.A, Okwoyo J.M and Giterere K, (2016), Numerical instigation of unsteady MHD free convective flow past an oscillating free vertical plate with oscillatory heat flux, *The Standard International Journal*,4(1),2321-2403.
4. Chepkemoi E. and Mukuna W.O. (2021). Hydromagnetic free convection unsteady turbulent fluid flow over a vertical infinite heat absorbing plate, *IOSR Journal of mathematics*, 17(3), 42-48.
5. Deka, R.K; Ashish, P; and Arun C. (2015). Transient free convection flow past a vertical cylinder with constant heat flux and mass transfer, *Ain Shams Engineering Journal* , <http://dx.doi.org/10.1016/j.asej.2015.10.006>.
6. Edward, J. S; Katz, I. M; and Scraff J. P.(2005). *Introduction to Fluid Mechanics*. Oxford University Press.
7. Holman, J. P. (2010). *Heat Transfer* (10th ed.). Mc Graw-Hill.
8. Incropera, F. (2007). *Fundamentals of Heat and Mass Transfer*. New Jersey: Wiley.
9. Kaya, A. (2011). Heat and mass transfer from horizontal slender cylinder with magnetic

field effect. *Journal of Thermal Science and Technology*, 31 (2), 73-78.

10. Kiprop K. (2017). Hydrodynamic radiating fluid flow past an infinite vertical porous plate in the presence of chemical reaction and induced magnetic field. *Jomo Kenyatta University of Agriculture and Technology*. Unpublished Msc thesis.
11. Kwanza, J.K; Mukuna, W.O; and Kinyanjui, M. (2010). A mathematical model of turbulent convective fluid flow past an infinite vertical plate with Hall current. *International Journal of Modelling and Simulation*, 30 (3), 376-386.
12. Loganathan, P; and Eswari, B.(2017). Natural convective flow over moving vertical cylinder with temperature oscillation in the presence of porous medium. *Global Journal of Pure and Applied Mathematics*, 13 (2), 839-855.
13. Masoud, A; Sina, N; Teimouri, H; Reza, M.S; Hemmat, M.E; Kamali, J; and Toghraie, D.(2015). Effect of magnetic field on free convection in inclined cylindrical annulus containing molten potassium. *International Journal of Applied Mechanics*, 7 (4), 1-16.
14. Mayaka J.O., Johana S., Kinyanjui M. (2014a). MHD turbulent flow in a porous medium with Hall current, Joule's heating and mass transfer. *International Journal of Science and Research*, 3(8), 2014.
15. Mc Comb W.D. (1992). *The Physics of Fluid Turbulence*. A clarendon press.
16. Mori, C.N; & Romdo, E.C. (2015). Numerical Simulation by Finite Difference Method

- of 2D convection Diffusion in Cylindrical equations. *Journal of Applied Mathematical Sciences*, 9 (123), 6157-6165.
17. Mukuna W.O. (2021) MHD turbulent free convection fluid flow over an infinite vertical heat generating cylinder, *International Advance Research Journal in science, Engineering and Technology*, 8(5),39-49.
18. Mukuna W.O., Chepkemoi E. and Rotich, J.K. (2020). Mathematical model of buoyancy driven hydromagnetic turbulent fluid flow over a vertical infinite plate using turbulent Prandtl number. *World Journal of engineering research and technology*, 6(5), 266-277.
19. Mukuna, W.O; Kwanza, J.K; Sigei, J.K; & Okello, J.A. (2017b). Analysis of heat and mass transfer rates of hydromagnetic turbulent fluid flow over an immersed cylinder with Hall current. *International Journal of Modelling and Simulation*, 7 (4), 45-64.
20. Mukuna, W.O; Kwanza, J.K; Sigei, J.K; and Okello, J.A. (2017a). Modelling hydromagnetic turbulent free convection fluid flow over an immersed infinite vertical cylinder. *World Journal of Engineering Research and Technology*, 3 (2), 218-234.
21. Odekeye, A.M; & Akirinmade, V. A. (2017). MHD mixed convection heat and mass transfer flow from vertical surfaces in porous media with Soret and Dufour effects. *Journal of Scientific and Engineering Reseach*, 4 (9), 75-85.
22. Pranton, R. L (2005). *Incompressible Flow* (3rd ed.). Wiley.

23. Rajesh, V; Anwar, B.R; and Sridevi, C. (2016). Finite difference analysis of unsteady MHD free convective flow over a moving semi-infinite vertical cylinder with chemical reaction and temperature oscillations. *Journal of Applied Fluid Mechanics*, 9 (1), 157-167.
24. Ravi, B. S; and Sambasiva, R.G. (2016). Bouyancy induced natural convective heat transfer along a vertical cylinder under constant heat flux. *International Journal of Chemical Science*, 9 (1), 157-167.
25. Sarris, E; Iatridis, A.I; Dritselis, C.D; and Vlachos, N.S. (2010). Magnetic field effect on the cooling of a low-Pr fluid in a vertical cylinder. *Physics of Fluids* , doi:10.63/1.3291074.
26. Seth Sarkar, G.S and Sharma R.(2016). Effects of hall current on unsteady hydromagnetic free convection flow past an impulsively moving vertical plate with Newtonian heating, *International Journal of Applied mechanics and Engineering*, 21(1), 187-203
27. Umameheswar, M; Raju, M.C; Varma S.V; and Gireeshkumar, J. (2016). Numerical investigation of MHD FREE convection of non-Newtonian fluid past an impulsively started vertical plate in the presence of thermal diffusion and radiation absorption. *Alexandrian Engineering Journal*, 55, 2005-2014.
28. Vijayalakshmi A.R and selva jayanthi M. (2018). Implicit scheme solution of unsteady MHD flow, *Applied mathematics and information sciences* 12(2), 379-388
29. Vishnu, N.G; Ganga, B; Hakeem, A; Saranya, S; and Kalaivanan, R. (2016).

Hydromagnetic asymmetrical slip flow over a vertical stretching cylinder with convective boundary. *St. Petersburg Polytechnicaal University Journal*, 2 (4), 273-280.

APPENDICES

Appendix I: MATLAB CODE

```
function MHD_TurbFlow()
clear all;clc;%close all;
global M m Pr Prt K Gr
z0=0;zInf=6;nz=150;dz=(zInf-z0)/(nz);
t0=0;tend=1;nt=2000;dt=(tend-t0)/(nt);
z=z0:dz:zInf;
t=t0:dt:tend;

%% parameters specification
M=2;      % 1.5, 2, 2.5;
Pr=3.5;   % 1.7, 3.5, 7;
Gr=-0.5;  % -1,-0.5, 0.5, 1
m=0.5;    % 0.2, 0.3, 0.5
color='--k'; % blue(b)-I,red(r)-II,black(k)-III,magenta(m)-IV;
Prt=0.85; K=0.4;

u=zeros(nz,nt);v=zeros(nz,nt);theta=zeros(nz,nt);
%% initial and boundary conditions
u(:,1)=0;v(:,1)=0;theta(:,1)=0;%IC

u(1,:)=1;v(1,:)=0;theta(1,:)=1;%BC at z=0
u(nz,:)=0;v(nz,:)=0;theta(nz,:)=0;%BC at z=Inf

%% implementation of Finite Difference Method
for j=1:nt
    for i=2:nz-1
        u(i,j+1)=u(i,j)+dt*Uvelocity(u(i+1,j),u(i,j),u(i-1,j),v(i+1,j),v(i,j),v(i-1,j),theta(i,j),i,dz);
        v(i,j+1)=v(i,j)+dt*Vvelocity(u(i+1,j),u(i,j),u(i-1,j),v(i+1,j),v(i,j),v(i-1,j),theta(i,j),i,dz);
        theta(i,j+1)=theta(i,j)+dt*Temp(theta(i+1,j),theta(i,j),theta(i-1,j),u(i+1,j),v(i,j),u(i-1,j),v(i+1,j),v(i-1,j),i,dz);
    end
end

%% plotting of the results
figure(1)
mesh(t(2:nt-1),z(2:nz-1),u(2:nz-1,2:nt-1))
figure(2)
mesh(t(2:nt-1),z(2:nz-1),v(2:nz-1,2:nt-1))
figure(3)
mesh(t(2:nt-1),z(2:nz-1),theta(2:nz-1,2:nt-1))
figure(4)
hold on
plot(z(1:nz),u(1:nz,nt),color,'linewidth',1)
xlabel('Distance Z');ylabel('Primary Velocity, U')
```

```

hold off
figure(5)
hold on
plot(z(1:nz),v(1:nz,nt),color,'linewidth',1)
hold off
xlabel('Distance Z');ylabel('Secondary Velocity, V')
figure(6)
hold on
plot(z(1:nz),theta(1:nz,nt),color,'linewidth',1)
hold off
xlabel('Distance Z');ylabel('Temperature, \theta')
%% prescription of the sub-functions
function URHS=Uvelocity(uij,uij,uimj,vipj,vij,vimj,thetaj,index,dz)
    URHS=(-(uij*vipj-uimj*vimj)/(2*dz))+((uij-
2*uij+uimj)/(dz*dz))+2*K*K*index*dz*((uij-uimj)/(2*dz))^2)...
    +2*K*K*((index*dz)^2)*((uij-2*uij+uimj)/(dz*dz))*((uij-
uimj)/(2*dz))+Gr*thetaj-M*M*(uij+m*vij)/(1+m*m);
end
function VRHS=Vvelocity(vipj,vipj,vimj,vimj,vipj,vij,vimj,thetaj,index,dz)
    VRHS=(-(vipj*vipj-vimj*vimj)/(2*dz))+((vipj-
2*vij+vimj)/(dz*dz))+2*K*K*index*dz*((vipj-vimj)/(2*dz))^2)...
    +2*K*K*((index*dz)^2)*((vipj-2*vij+vimj)/(dz*dz))*((vipj-
vimj)/(2*dz))+Gr*thetaj-M*M*(vij-m*uij)/(1+m*m);
end
function
TRHS=Temp(thetaj,thetaj,thetaj,uij,vij,uimj,vipj,vimj,index,dz)
    TRHS=(-(thetaj*vipj-thetaj*vimj)/(2*dz))+1/Pr*((thetaj-
2*thetaj+thetaj)/(dz*dz))...
    -2*K*K*((index*dz)^2)*1/Pr*((uij-uimj)/(2*dz))*((thetaj-
thetaj)/(2*dz));
end
end

```

Appendix II: Clearance to commence field work



UNIVERSITY OF KABIANGA
ISO 9001:2015 CERTIFIED

OFFICE OF THE DIRECTOR, BOARD OF GRADUATE STUDIES

REF: PGC/AM/0002/17

DATE: 21ST SEPTEMBER, 2021

Wesley Cheruiyot Kemboi,
MAPS,
University of Kabianga,
P.O Box 2030- 20200,
KERICHO.

Dear Mr. Kemboi,

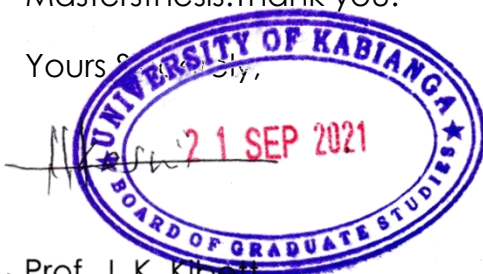
RE: CLEARANCE TO COMMENCE FIELD WORK

I am glad to inform you that the Board of Graduate Studies during its meeting on 14th July 2021 approved your research proposal entitled “**Modeling and Analysis of Magnetohydrodynamic Free Convection Turbulent Fluid Flow Past an Infinite Vertical Porous Plate**”.

I am also acknowledging receipt of your corrected proposal via email and hard copies. You are now free to commence your field work on condition that you obtain a research permit from NACOSTI.

Please note that, you are expected to publish at least one (1) paper in a peer reviewed journal before final examination (oral defense) of your Mastersthesi. Thank you.

Yours Sincerely,



Prof. J. K. Kibet
DIRECTOR, BOARD OF GRADUATE STUDIES.

JKK/hk

CC:-

1. Dean, SST
2. HOD, MAPS
3. Supervisors



MODELING AND ANALYSIS OF MAGNETOHYDRODYNAMIC FREE CONVECTION TURBULENT FLUID FLOW PAST A VERTICAL INFINITE POROUS PLATE

W. C. Kemboi¹, W.O. Mukuna^{1*} and J.K. Rotich¹

Department of Mathematics, Actuarial and Physical Sciences, University of Kabianga, P.O. Box 2030-20200,
Kericho, Kenya¹

Abstract: A mathematical model of a two-dimension magnetohydrodynamic (MHD) free convection fluid flow that is turbulent and past a vertical infinite porous plate is developed. The fluid flow is impulsively started to in x-direction. Flow problem modeled using conservation of momentum, and conservation of energy equations. The arising partial differential equations, which are nonlinear, are solved numerically using explicit finite difference scheme. Simulation of the discretized equations is done using MATLAB. The impacts of flow parameters on velocities and temperature profiles such as Magnetic parameter (M), Hall parameter (m), and Prandtl number (Pr) were examined. It is evident from the results that during the cooling of the plate ($Gr > 0$), the primary velocity decreases with decrease in Hall parameter, m , and increase in magnetic parameter, M . It also decreases as the prandtl number, Pr , is increased. The secondary velocity decreases with decrease in Hall parameter, m , and increase in magnetic parameter, M . It also decreases as the prandtl number, Pr is increased. The results also shows that there is no significant effect on temperature profile as the Hall parameter is decreased. There is also no significant change as the magnetic parameter is increased. It is also evident that there is a decrease in temperature profile when the Prandtl number is increased.

Key words: Porous plate, Free Convection, Magnetohydrodynamic, Turbulent, Finite difference

LIST OF SYMBOL

H	Magnetic field intensity, (Wb/m^2)
B	Magnetic flux density, (Wb/m^2)
J	Current density vector
E	Electric field (V/m^3)
H_0	Constant magnetic field intensity, Wb/m^2
u, v, w	Velocity components in the x, y , and z direction respectively, m/s
u', v', w'	Fluctuating components of velocity
$\bar{u}, \bar{v}, \bar{w}$	Mean velocities
a	Acceleration, (m/s^2)
Q	Heat, (J)
W	Work, (J)
p	Fluid pressure, N/m^2
g	Acceleration due to gravity, m/s^2
t	Time, s
T	Absolute temperature, K
C_p	Specific heat at constant pressure of the fluid, $J/kg/K$
Re	Reynolds number
L	Characteristic length, m
M	Magnetic parameter
Pr	Prandtl number
Gr	Grashoff number
Ec	Eckert number



Rt	Time parameter
μ	Coefficient of viscosity, kg/ms
ρ	Fluid density, kg/m^3
α	Coefficient of thermal diffusivity, m^2/s
ν	Coefficient of kinematic viscosity, m^2/s
σ	Electrical conductivity, $\Omega^{-1}m^{-1}s$
β	Coefficient of thermal expansion, K^{-1}

I. INTRODUCTION

Many researchers have done investigations on magnetohydrodynamics which of great interest to scientists and engineers. Several investigations both theoretical and experimental have been done in the past in relation to this. Mukuna *et al.* (2020) modeled a Hydromagnetic free convection turbulent fluid flow over a vertical infinite plate using turbulent Prandtl number. Vijayalakshmi *et al.* (2018) did a research on the unsteady electrically transmitting fluid past an oscillating semi- infinite vertical plate with uniform temperature and mass diffusion under chemical reactions. Odekeye and Akinrinmade (2017) did a MHD research on mixed convective heat and mass transfer flow from vertical surfaces in porous media with Soret and Dufour effects. Loganathan and Eswari (2017) did a research on natural convective flow over moving vertical cylinder with temperature oscillation in the presence of porous medium. They used the iterative tridiagonal semi-implicit finite difference method. Mukuna *et al.* (2017b) analyzed heat and mass transfer rates of hydromagnetic turbulent fluid flow over an immersed cylinder with Hall current.

They modeled the flow using conservation equations and solved the arising partial differential equations using finite difference scheme. Mukuna *et al.* (2017a) researched on hydromagnetic turbulent free convection fluid flow over an immersed infinite vertical cylinder, modeled their problem using conservation equations and later solved the arising partial differential equations using finite difference scheme. Kiprop (2017) did a research on an unsteady MHD flow with mass and heat transfer in an incompressible, viscous, Newtonian and electrically conducting fluid past a vertical porous plate with consideration of chemical reaction, thermal radiation and induced magnetic field. Solution of governing equations were done using finite difference scheme, that is the Crank- Nicholson method. Seth *et al.* (2016) studied on the effects of an unsteady free convection flow past an impulsively moving porous vertical plate with Newtonian heating. Chebos *et al.* (2016) investigated an unsteady MHD free convection flow past an oscillating vertical porous plate with oscillatory heat flux. It is worth noting that despite of all these, MHD turbulent fluid flow has received little attention as expected.

The main objective of the present research is to study a two-dimensional hydro magnetic free convective flow of an incompressible viscous and electrically conducting fluid flow that is turbulent and past a vertical infinite porous plate using a mathematical model. It is evident from the results that during both the cooling and Heating of the plate ($Gr > 0$ and $Gr < 0$), the primary velocity decreases with decrease in Hall parameter, m , and increase in magnetic parameter, M . It also decreases during cooling of the plate as the prandtl number, Pr , is increased and even during the heating of the plate as the prandtl number, Pr , is decreased. For $Gr > 0$ and $Gr < 0$, the secondary velocity decreases with decrease in Hall parameter, m , and increase in magnetic parameter, M . It also decreases during cooling of the plate as the prandtl number, Pr is increased and also during heating of the plate as the prandtl number, Pr is decreased. The results also shows that there is NO significant effect on temperature profile during both cooling and heating of the plate as the Hall parameter is decreased. There is also NO significant change during the cooling of the plate as the magnetic parameter is increased and even during the heating of the plate as the magnetic parameter is decreased. It is also evident that there is a decrease in temperature profile when the Prandtl number is increased in both the cooling and Heating of the plate.

II. MATHEMATICAL MODEL

A two-dimensional flow is considered in this study. The infinite vertical porous plate is taken to be along the x-axis and the y-axis taken to be on the horizontal whereas the z-axis normal to the plate. The fluid being considered is incompressible and viscous. A magnetic field of a high magnitude H_0 is applied perpendicularly to the direction of flow of the fluid. It is assumed that the induced magnetic field is negligible therefore $H = (0,0,H_0)$ as indicated in the diagram below. At time $t^* > 0$, the fluid is stationary and the plate starts to move impulsively in its plane with velocity



U_0 and the temperature of the plate raised instantly to T_w^* and maintained constant later on. The schematic diagram for the fluid flow is as given below:

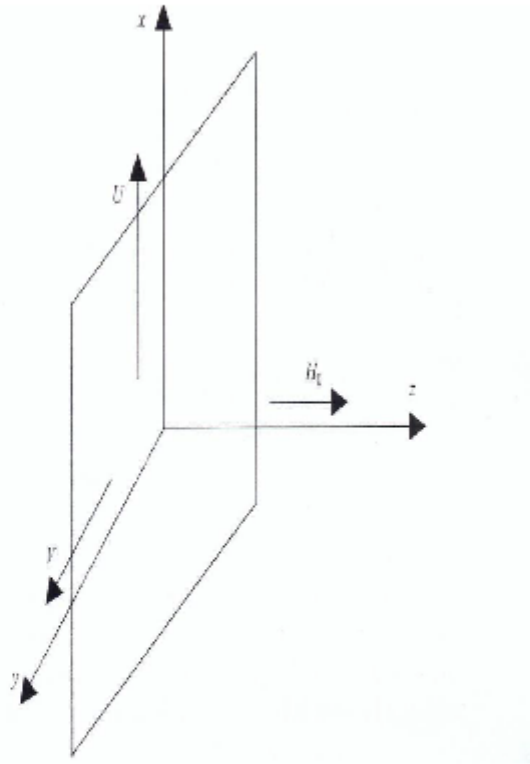


Figure 1: Schematic diagram for the fluid flow.

The flow is therefore governed by the following equations:

$$\frac{\partial U^*}{\partial t^*} + V^* \frac{\partial U^*}{\partial y^*} = -\frac{1}{\rho} \frac{\partial p}{\partial x} + \nu \left(\frac{\partial^2 U^*}{\partial x^{*2}} \right) - \frac{\partial(\overline{uw})}{\partial x^*} + \rho g + JxB \tag{1}$$

$$\frac{\partial V^*}{\partial t^*} + V^* \frac{\partial V^*}{\partial y^*} = \nu \left(\frac{\partial^2 V^*}{\partial x^{*2}} \right) - \frac{\partial(\overline{vw})}{\partial x^*} + JxB \tag{2}$$

$$\frac{\partial T^*}{\partial t^*} + V^* \frac{\partial T^*}{\partial y^*} = \frac{k}{\rho C_p} \left(\frac{\partial^2 T^*}{\partial x^{*2}} \right) - \frac{\partial(\overline{wT^*})}{\partial x^*} \tag{3}$$

Where $\nu = \frac{\mu}{\rho}$ is the kinematic viscosity

ρ is the fluid density

The initial and boundary conditions will be as follows:

$$t^* > 0 : U^* = 0, V^* = 0, T^* = T_{\infty}^* \text{ everywhere} \tag{4a}$$

$$t^* \geq 0 : U^* = 0, V^* = 0, T^* = T_w^* \text{ at } z = 0; \tag{4b}$$



$$U^* \rightarrow U_0, V^* \rightarrow 0, T^* \rightarrow T_{\infty}^* \text{ as } z \rightarrow \infty \tag{4c}$$

On introducing non dimensional quantities:

$$t = \frac{t^* U_0^2}{\nu}, \quad z = \frac{z^* U_0}{\nu}, \quad U = \frac{U^*}{U_0}, \quad V = \frac{V^*}{U_0}, \quad \theta = \frac{T^* - T_{\infty}^*}{T_w^* - T_{\infty}^*},$$

$$Gr = \frac{\nu g \beta (T_w^* - T_{\infty}^*)}{U_0^3}, \quad \theta = \frac{T^* - T_{\infty}^*}{T_w^* - T_{\infty}^*}, \quad M^2 = \frac{\sigma \mu_0^2 H_0^2 \nu}{U_0^2}$$

The above governing equations and boundary conditions becomes:

$$\frac{\partial U}{\partial t} + V \frac{\partial U}{\partial y} = \left(\frac{\partial^2 U}{\partial z^2} \right) - \frac{\partial \overline{u\overline{w}}}{\partial z} - Gr\theta + \frac{M^2(mV-U)}{(1+m^2)} \tag{5}$$

$$\frac{\partial V}{\partial t} + V \frac{\partial V}{\partial y} = \left(\frac{\partial^2 V}{\partial z^2} \right) - \frac{\partial \overline{v\overline{w}}}{\partial z} - \frac{M^2(mU+V)}{1+m^2} \tag{6}$$

$$Pr \left(\frac{\partial \theta}{\partial t} + V \frac{\partial \theta}{\partial y} \right) = \left(\frac{\partial^2 \theta}{\partial z^2} \right) - Pr \frac{\partial \overline{w\overline{T}}}{\partial z} \tag{7}$$

$$t < 0, U = 0, V = 0, \theta = 0, \text{ everywhere} \tag{8a}$$

$$t \geq 0, U = 0, V = 0, \theta = 0, \text{ at } z \rightarrow \infty \tag{8b}$$

$$U = 1, V = 0, \theta = 1, \text{ at } z = 0 \tag{8c}$$

III. PRANDTL MIXING LENGTH HYPOTHESIS

It is not possible to solve these equations due to the existence of the Reynolds stresses $\overline{u\overline{w}}$ and $\overline{v\overline{w}}$ in equations (5) and (6) respectively, therefore the need to adopt the Boussinesque approximation

$$\tau_t = -\rho \overline{u\overline{v}} = A_t \frac{dU}{dy} \tag{9}$$

It is worth noting that A_t is not a fluid property as μ but depends on mean velocity U . On the other hand, $\rho \overline{u\overline{v}}$ stands for flux of x-momentum in the y-direction, which is assumed that this momentum was transported by eddies which moved in the y-direction over a given distance say l with no interaction and then mixed with the existing fluid at the new location i.e momentum is taken to be conserved over distance l , (McComb, 1990).

Prandtl was able to deduce experimentally that:

$$\rho \overline{u\overline{v}} = -\rho l^2 \left(\frac{\partial U}{\partial y} \right)^2 \tag{10}$$

At this level, more assumptions are taken as follows:

- i) $y^+ > 5$, viscous term in shear stress is neglected.
- ii) $l = ky$, where k is the karman constant given as $k = 0.4$, McComb, (1990).

On substituting l^2 , it yields

$$\rho \overline{u\overline{v}} = \rho k^2 y^2 \left(\frac{\partial U}{\partial y} \right)^2 \text{ This reduces to}$$

$$\overline{u\overline{v}} = -k^2 y^2 \left(\frac{\partial U}{\partial y} \right)^2 \tag{11}$$

Equation 4.46 can be deduced further to give

$$\overline{u\overline{w}} = -k^2 z^2 \left(\frac{\partial U}{\partial z} \right)^2 \tag{12}$$

And

$$\overline{v\overline{w}} = -k^2 z^2 \left(\frac{\partial V}{\partial z} \right)^2 \tag{13}$$



Considering the turbulent Prandtl number also given by

Pr_t = epsilon_M / epsilon_H where epsilon_M = -2k^2 z^2 du/dz

Thus,

It can be deduced from (11) that W_T = (-2k^2 z^2 du/dz) / epsilon_M (14)

It can now be shown that equations (11),(12), (13) and (14) can yield the following set of differential equations as:

du/dt + V du/dy = (d^2u/dx^2) + 2k^2 z (du/dz)^2 + 2k^2 z^2 (d^2u/dx^2) (du/dz) + Gr theta + M^2(mU+V)/(1+m^2) (15)

dV/dt + V dV/dy = (d^2V/dx^2) + 2k^2 z (dV/dz)^2 + 2k^2 z^2 (d^2V/dx^2) (dV/dz) - M^2(mV-U)/(1+m^2) (16)

Pr (d theta/dt + V d theta/dy) = (d^2 theta/dx^2) + Pr ((2k^2 z^2 du/dz) / Pr_t) (d theta/dz) (17)

IV. EXPLICIT FINITE DIFFERENCE SCHEME

The explicit finite difference scheme is employed in the solution of these governing equations (15), (16) and (17) since they are highly non-linear. The approximations of these governing equations using the Finite difference Scheme are respectively given where

In this case, k = 0.4, z = i delta x and i and j refer to z and t respectively.

The initial and boundary conditions will now take the form given as:

U_i,j = 0; V_i,j = 0; theta_i,j = 0 Everywhere for theta < 0 (18a)

theta >= 0; U_i,j = 0; V_i,j = 0; theta_i,j = 1 For i = 0 (18b)

U_i,j = 1; V_i,j = 0; theta_i,j = 0 For i = infinity (18c)

The computation for the consecutive grid points for primary and secondary velocity and temperature can now be done using the initial and boundary conditions i.e:

U_{(i,j+1)}; V_{(i,j+1)} and theta_{(i,j+1)}
U_{(i,j+1)} = U_{(i,j)} + delta t { -V_{(i,j)} (U_{(i+1,j)} - U_{(i,j)}) / delta y + (U_{(i+1,j)} - 2U_{(i,j)} + U_{(i-1,j)}) / (delta x)^2 + 0.32 i delta z (U_{(i+1,j)} - U_{(i,j)})^2 + 0.32 (i delta z)^2 (U_{(i+1,j)} - 2U_{(i,j)} + U_{(i-1,j)}) / (delta z)^2 (U_{(i,j)} - U_{(i-1,j)}) + Gr theta_{i,j} + M^2 (mV_{(i,j)} - U_{(i,j)}) / (1+m^2) } (19)

V_{(i,j+1)} = V_{(i,j)} + delta t { -V_{(i,j)} (V_{(i+1,j)} - V_{(i,j)}) / delta y + (V_{(i+1,j)} - 2V_{(i,j)} + V_{(i-1,j)}) / (delta x)^2 + 0.32 i delta z (V_{(i+1,j)} - V_{(i,j)})^2 + 0.32 (i delta z)^2 (V_{(i+1,j)} - 2V_{(i,j)} + V_{(i-1,j)}) / (delta z)^2 (V_{(i,j)} - V_{(i-1,j)}) + Gr theta_{i,j} + M^2 (mU_{(i,j)} + V_{(i,j)}) / (1+m^2) } (20)

theta_{i,j+1} = theta_{(i,j)} + delta t { -V_{i,j} (theta_{(i+1,j)} - theta_{i,j}) / delta y + 1/Pr [(theta_{(i+1,j)} - 2theta_{(i,j)} + theta_{(i-1,j)}) / (delta z)^2 + 0.32 (i delta z)^2 Pr / Pr_t ((U_{(i+1,j)} - U_{(i,j)}) / delta x) (theta_{(i+1,j)} - theta_{(i,j)})] } (21)

V. DISCUSSION OF RESULTS

For physical understanding of the problem and discussion of results, numerical simulation has been run for velocity and temperature profiles. Graphical presentation of the numerical results of the discretized governing equations from MATLAB is given. Various fluid parameters were varied on primary velocity, U, secondary velocity, V, and temperature, theta, profiles and then discussed. The effects of flow parameters including Grashoff numbers, Gr, Prandtl number, Pr, magnetic parameter, M, and Hall parameter, m, on mean primary velocity, U, secondary velocity, V, and temperature profile, theta, obtained. In each case, Pr_t = 0.85, and K = 0.4.

From figure 2, it can be shown that Hall current has little significance to primary velocity. However, primary velocity decreases with decrease in Hall parameter. This may be attributed to the fact that for a small value of m, the term 1/(1+m) will in turn increases the resistive force of the applied magnetic parameter thus reducing the primary velocity.



Figure 3 clearly shows that primary velocity decreases with increase in magnetic parameter. Magnetic parameter, M , refers to the ratio of the magnetic force to inertial force therefore higher M means higher magnetic force acting perpendicularly on an electrically conducting fluid hence developing Lorentz force which is an opposing force to fluid motion thus decreasing the primary velocity.

Considering figure 4, primary velocity decreases with increase in Prandtl number, Pr , though in a smaller extent. This is because increased Prandtl number leads to increase in viscosity making the fluid more thick thus leading to a decrease in primary velocity.

Figure 5 shows a significant decrease in secondary velocity with decrease in Hall parameter, m . Considering the model equation, and the fact that for any value of m , in the term $\frac{1}{1+m^2}$ will decrease the negative value of M^2 which will in turn decrease the secondary velocity.

It can also be clearly shown From figure 6 that secondary velocity was increased first at the beginning but later decrease with an increase in magnetic parameter, M . This is because at the beginning, Lorentz force decelerated the primary velocity but increased the lateral flow which in this case is the secondary velocity. The secondary velocity later decreased with increase in magnetic parameter because of the reduction of the magnetic force by the Hall current. Clearly, figure 7 depicts a decrease in secondary velocity with an increase in Prandtl number. This is due to increased viscosity of the fluid hence decreasing the secondary velocity.

Figure 8 clearly shows that there is no significant change in temperature as the Hall parameter is varied. However, the small change shows that the temperature, θ , of the fluid flow decreases with decrease in Hall parameter.

From figure 9, it shows there is no significant temperature change with variation in magnetic parameter. However, the small change indicates that there is a decrease in temperature profile with increase in magnetic parameter.

Figure 10 shows that there is a decrease in temperature profile with an increase in prandtl number . since prandtl number is the ratio of momentum diffusivity to thermal diffusivity, thus increased prandtl number means lower thermal diffusivity in comparison to momentum diffusivity hence decreasing thermal boundary layer which will in turn decreases the temperature distribution of the fluid.

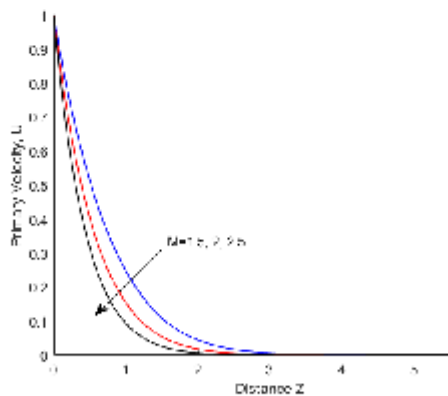


Figure 2: Variation of M on Primary Velocity Profiles

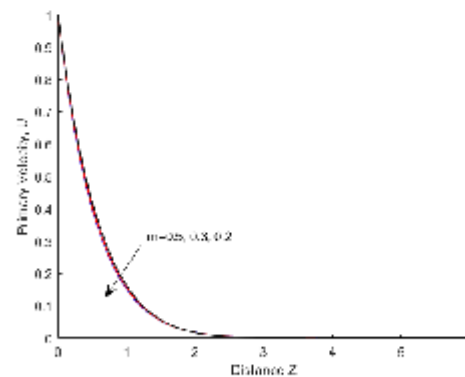


Figure 3: Variation of m on Primary Velocity Profiles

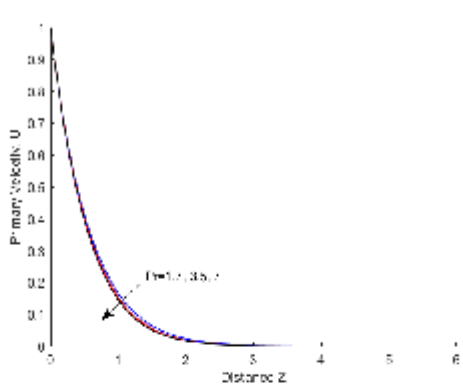


Figure 4 Variation of Pr on Primary Velocity Profiles

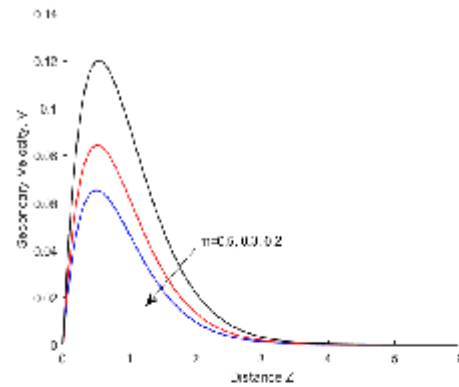


Figure 5 Variation of m on Secondary Velocity Profiles

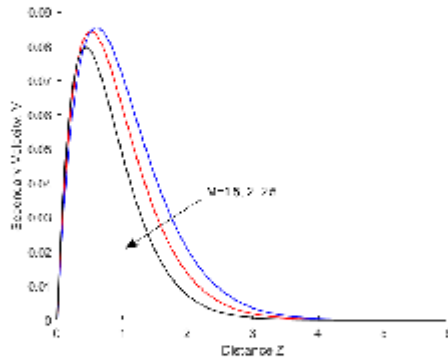


Figure 6 Variation of M on Secondary Velocity Profiles

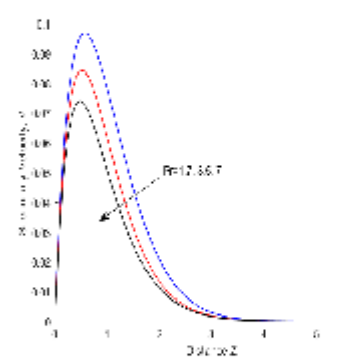


Figure 7 Variation of Pr on Secondary Velocity Profiles

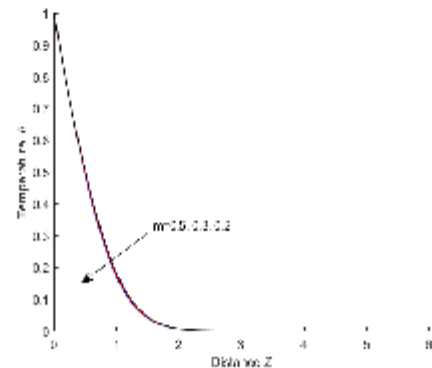


Figure 8: Variation of m on Temperature Profiles

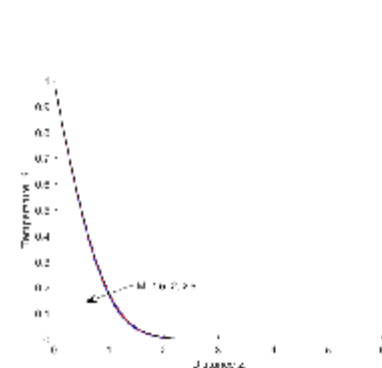


Figure 9: Variation of M on Temperature Profiles

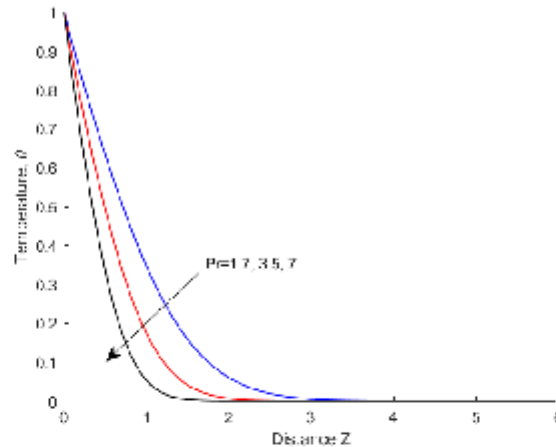


Figure 10: Variation of Pr on Temperature Profiles

VI. VALIDATION OF RESULTS

Our results when compared with those of Kwanza *et al.* (2010) who developed a mathematical model of turbulent convective fluid flow past an infinite vertical plate with Hall current in a dissipative fluid and found out that an increase in hall current leads to an increase in velocity profiles. These results are in agreement with our results. Comparison also with Mukuna *et al.* (2020) who modeled a Hydromagnetic free convection turbulent fluid flow over a vertical infinite plate using turbulent Prandtl number. They found out that there is an increase in primary velocity whenever magnetic parameter (M) is decreased, Hall parameter increased and when Grashoff number is increased.

It was also evident that secondary velocity increases when magnetic parameter (M) is decreased and decreases when Hall parameter is increased. They also found out that temperature profile decreases when magnetic parameter (M) is decreased, decreases when Hall parameter is increased and also increases when Prandtl number decreases. These results also agree with the findings of this paper.

VII. CONCLUSION

The method of solution used in this paper which is explicit finite difference scheme has made it possible to approximate the solution to the highly non linear partial differential equations. The simulation was done using MATLAB and the discussed results are summarised as:

- i) During the cooling of the plate ($Gr > 0$), the primary velocity decreases with decrease in Hall parameter, m , and increase in magnetic parameter, M . It also decreases as the Prandtl number, Pr , is increased.
- ii) During the cooling of the plate ($Gr > 0$), the secondary velocity decreases with decrease in Hall parameter, m , and increase in magnetic parameter M . It also decreases as the Prandtl number, Pr , is increased.
- iii) There is no significant effect on temperature profile, θ , during the cooling of the plate as the Hall parameter, m , is decreased. There is also no significant change as the magnetic parameter, M , is increased. There is decrease in temperature profile when Prandtl number, Pr , is increased.



REFERENCES

- [1] Chebos C., J.K Sigey, J.A okelo, J.M. Okwoyo and K. Giterere (2016), Numerical instigation of unsteady MHD free convective flow past an oscillating free vertical plate with oscillatory heat flux, *The Standard International Journal*, 4(1), 2321-2403.
- [2] Chepkemoi E. and Mukuna W.O. (2021). Hydromagnetic free convection unsteady turbulent fluid flow over a vertical infinite heat absorbing plate, *IOSR Journal of mathematics*, 17(3), 42-48.
- [3] Kwanza, J.K; Mukuna, W.O; and Kinyanjui, M. (2010). A mathematical model of turbulent convective fluid flow past an infinite vertical plate with Hall current. *International Journal of Modelling and Simulation*, 30 (3), 376-386.
- [4] Loganathan, P; and Eswari, B.(2017). Natural convective flow over moving vertical cylinder with temperature oscillation in the presence of porous medium. *Global Journal of Pure and Applied Mathematics*, 13 (2), 839-855.
- [5] Mukuna W.O. (2021) MHD turbulent free convection fluid flow over an infinite vertical heat generating cylinder, *International Advance Research Journal in science, Engineering and Technology*, 8(5),39-49.
- [6] Mukuna W.O., Chepkemoi E. and Rotich, J.K. (2020). Mathematical model of buoyancy driven hydromagnetic turbulent fluid flow over a vertical infinite plate using turbulent Prandtl number. *World Journal of engineering research and technology*, 6(5), 266-277.
- [7] Mukuna, W.O; Kwanza, J.K; Sigey, J.K; & Okello, J.A. (2017). Analysis of heat and mass transfer rates of hydromagnetic turbulent fluid flow over an immersed cylinder with Hall current. *International Journal of Modelling and Simulation*, 7 (4), 45-64.
- [8] Mukuna, W.O; Kwanza, J.K; Sigey, J.K; and Okello, J.A. (2017). Modelling hydromagnetic turbulent free convection fluid flow over an immersed infinite vertical cylinder. *World Journal of Engineering Research and Technology*, 3 (2), 218-234.
- [9] Odekeye, A.M; & Akirinmade, V. A. (2017). MHD mixed convection heat and mass transfer flow from vertical surfaces in porous media with Soret and Dufour effects. *Journal of Scientific and Engineering Reseach*, 4 (9), 75-85.
- [10] Rajesh, V; Anwar, B.R; and Sridevi, C. (2016). Finite difference analysis of unsteady MHD free convective flow over a moving semi-infinite vertical cylinder with chemical reaction and temperature oscillations. *Journal of Applied Fluid Mechanics*, 9 (1), 157-167.
- [11] Ravi, B. S; and Sambasiva, R.G. (2016). Bouyancy induced natural convective heat transfer along a vertical cylinder under constant heat flux. *International Journal of Chemical Science*, 9 (1), 157-167.
- [12] Seth, G. S. Sarkar and Sharma R.(2016). Effects of hall current on unsteady hydromagnetic free convection flow past an impulsively moving vertical plate with Newtonian heating, *International Journal of Applied mechanics and Engineering*, 21(1), 187-203